Journal of Sound and Vibration (1999) **222**(3), 453–487
Article No. jsvi1998.2065, available online at http://www.idealibrary.com on IDEAL

ONE-DIMENSIONAL WAVE PROPAGATION IN A FUNCTIONALLY GRADED ELASTIC MEDIUM

T.-C. CHIU AND F. ERDOGAN
Department of Mechanical Engineering and Mechanics, Lehigh University, Bethlehem, PA 18015, *U.S.A.*

(*Received* 24 *November* 1997, *and in final form* 23 *November* 1998)

In this study the one-dimensional wave propagation in a functionally graded elastic slab is considered. It is assumed that the stiffness and density of the medium vary continuously in thickness direction and it is initially at rest and stress-free. The slab is subjected to a pressure pulse on one surface and a vanishing stress or displacement condition on the other. The solution is obtained in wave summation form. Propagation of a rectangular pressure pulse in a graded medium that consists of either nickel/zirconia or aluminum/silicon carbide is studied as examples. It is shown that there is considerable wave distortion in time and the distortion is much more pronounced in slabs with fixed/free boundary conditions. A simple approximate expression giving the peak stress is developed. Also it is demonstrated that the energy balance principle may be used as a convergence criterion in the calculation of stresses.

1. INTRODUCTION

Within the past decade there has been considerable interest in grading the thermomechanical properties of particulate composites as a tool for designing new materials for specific applications. Most of the research in this area involves the development of graded coatings and interfacial regions for the purpose of reducing residual and thermal stresses and increasing the bonding strength (see references [1–4] for review and further references). Such particulate composites with continuously varying volume fractions are known as functionally graded materials (FGMs). Aside from the thermal barrier coatings, some of the potential applications of FGMs include manufacturing of wear-resistant components such as gears, cams, bearings, and machine tools. Regardless of the fields of application, generally the dominant modes of failure in FGM coatings and interlayers appear to be cracking and spallation. In addition to the appropriate fracture mechanics, dealing with these failure problems requires a detailed stress analysis for identifying the likely sites of failure initiation and for determining the peak values of stresses. In some cases the loading of these inhomogeneous components may be dynamic in nature. Thus, an important area of interest in considering the applications of graded materials would be to study the dynamic response of the component to, for example, impact or blast loading.

0022–460X/99/180453 + 35 $30.00/0

In elastodynamics of materials with continuously varying properties, usually the pulse shape is distorted in time, the wave propagation speed is not constant, and there are no sharp interfaces that would cause wave reflections. Consequently, even in the simple case of one-dimensional wave propagation the locations and magnitudes of peak stresses cannot be determined by inspection.

Because of its relevance in geophysics and soil mechanics, in the past there has been quite considerable interest in the elastodynamics of inhomogeneous media. In 1946 Friedlander [5] proposed a solution that consists of a series of terms the first of which describes the wave motion predicted by geometrical optics and the subsequent terms account for certain types of diffraction effects. Karal and Keller [6] extended this method to treat general wave propagation problems in inhomogeneous elastic media by formulating the problem in terms of displacements and displacement potentials. Pekeris [7] used an asymptotic method to solve the problem for a half space with a variable speed of sound and reduced the solution to a Fourier–Bessel series. Scholte [8], who allowed for arbitrary variation in speed of sound and density, obtained a solution by using a successive approximations technique in which the sequence of terms obtained correspond to the direct wave, single reflections, and multiple reflections of successive order. Gupta [9] obtained a solution involving Bessel functions of imaginary order for the Helmholtz equation with linear variation of the wave speed in depth. Lindholm and Doshi [10] considered a slender bar with free/free ends and variable Young's modulus and obtained a solution that is synthesized from the eigenfunctions by using the principle of virtual work. Reiss [11, 12] considered the Klein–Gordon equation and obtained an asymptotic solution.

To solve the initial value problems arising from the wave propagation in elastic solids, a widely used technique is that of Laplace transforms. Whittier [13] treated the problem that was considered by Lindholm and Doshi [10] by using Laplace transforms and gave an asymptotic solution. Similarly, Payton [14] considered a semi-infinite rod subjected to a pressure step at its end with several different wave speeds. Steele [15] developed an asymptotic solution for a semi-infinite elastic slab which was subjected to an impulsive loading and had a Young's modulus varying in depth direction. Yedlin *et al.* [16] considered the wave equation for a semi-infinite medium in which both Young's modulus and density are allowed to vary smoothly in depth direction. Karlsson *et al.* [17] developed a Green's function approach for one-dimensional transient wave propagation in composite materials. Instead of assuming the material parameters to be continuous functions, one may assume the composite to be a multilayered medium having piecewise constant properties. Because of its application to layered composites, in the past the elastodynamics of such piecewise homogeneous materials has also attracted considerable attention (see for example, references [18–20]). There are also purely numerical techniques to treat the problem of wave propagation in inhomogeneous solids. For example, Pai [21] used the method of generalized Haskell matrix to solve the one-dimensional wave equation, whereas Harker and Ogilvy [22] used a finite difference technique to obtain the solution of the coherent wave propagation problem for inhomogeneous materials.

In this study we consider the one-dimensional problem in elastodynamics for an FGM plate in which material properties vary only in thickness direction. The boundary conditions are assumed to be either free/free or fixed/free. The Laplace transform technique is used to solve the problem. Even though the technique could accommodate arbitrary inputs, the problem is solved under zero initial conditions with a rectangular pressure pulse as the external load.

2. FORMULATION OF THE PROBLEM

The one-dimensional elastodynamic problem under consideration is described in Figure 1. It is assumed that the slab is isotropic and inhomogeneous with the following fairly general properties:

$$E'(x) = E'_o\left(a\frac{x}{l}+1\right)^m, \qquad \rho(x) = \rho_o\left(a\frac{x}{l}+1\right)^n, \tag{1a, b}$$

where ρ is the mass density, l is the thickness, a, m, and n are arbitrary real constants with $a > -1$, E'_o and ρ_o are the elastic constant and density at $x = 0$, and the elastic constant E' is determined under the assumption that $\sigma_{yy} = \sigma_{zz}$ and the slab is fully constrained at infinity. It can thus be shown that

$$E' = \frac{E(1-\nu)}{(1+\nu)(1-2\nu)}, \tag{2}$$

$E(x)$ and $v(x)$ being the Young's modulus and the Poisson's ratio of the inhomogeneous material. Note that the displacement components u_y and u_z are zero, and the stress state is one-dimensional and is given by

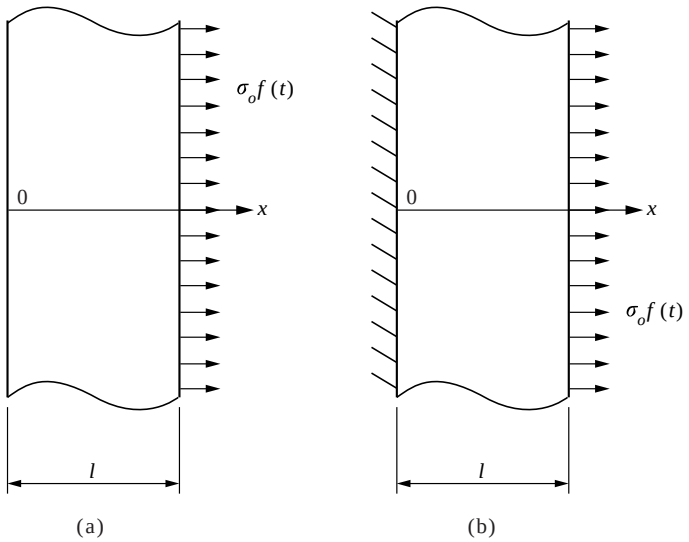

Figure 1. Boundary conditions and loading for an FGM slab; (a) free/free, (b) fixed/free boundaries, $\sigma_{xx}(l, t) = \sigma_o f(t)$ stress pulse.

$$\sigma_{xx} = E' \frac{\partial u}{\partial x}, \tag{3}$$

where the unknown function $u(x, t) = u_x(x, t)$ must satisfy the following wave equation:

$$\frac{\partial}{\partial x}\left(E'(x)\frac{\partial u}{\partial x}\right) = \rho(x)\frac{\partial^2 u}{\partial t^2}. \tag{4}$$

Assuming that the slab is at rest for $t \leqslant 0$, equation (4) must be solved under the following initial conditions:

$$u(x, 0) = 0, \qquad \frac{\partial}{\partial t}u(x, 0) = 0, \qquad 0 < x < l. \tag{5a, b}$$

Now introducing the normalized quantities

$$X = x/l, \qquad T = c_o t/l, \qquad U = u/l, \qquad c_o = \sqrt{E_o'/\rho_o}, \tag{6}$$

from equations (1), (4), and (5) it may be shown that

$$\frac{\partial}{\partial X}\left[(aX+1)^m \frac{\partial U}{\partial X}\right] = (aX+1)^n \frac{\partial^2 U}{\partial T^2}, \tag{7}$$

$$U(X, 0) = 0, \qquad \frac{\partial}{\partial T}U(X, 0) = 0. \tag{8}$$

By using the standard Laplace transform with respect to normalized time T, the solution of equation (7) may be expressed as

$$U(X, T) = \frac{1}{2\pi i}\int_{c-i\infty}^{c+i\infty} \hat{U}(X, p)e^{pT}\, dp, \tag{9}$$

where the differential equation to determine $\hat{U}$ is obtained from equations (7) and (8) as follows:

$$\eta^2 \frac{d^2\hat{U}}{d\eta^2} + m\eta\frac{d\hat{U}}{d\eta} - \frac{p^2}{a^2}\eta^{n-m+2}\hat{U} = 0, \qquad \eta = (aX+1). \tag{10a, b}$$

Equation (10) can be solved in closed form, giving

$$\begin{aligned}\hat{U}(X, p) = (aX+1)^{\frac{1-m}{2}}\Bigg[&C_1 \cdot \mathrm{I}_{\left|\frac{1-m}{n-m+2}\right|}\left(\left|\frac{2p}{(n-m+2)a}\right|(aX+1)^{\frac{n-m+2}{2}}\right)\\ &+C_2 \cdot \mathrm{K}_{\left|\frac{1-m}{n-m+2}\right|}\left(\left|\frac{2p}{(n-m+2)a}\right|(aX+1)^{\frac{n-m+2}{2}}\right)\Bigg]\end{aligned} \tag{11a}$$

for $m \neq n+2$ and

$$\hat{U}(X, p) = C_3(aX+1)^{s_3} + C_4(aX+1)^{s_4} \tag{11b}$$

for $m = n + 2$, where

$$s_3, s_4 = -\frac{n+1}{2} \pm \sqrt{\left(\frac{n+1}{2}\right)^2 + \left(\frac{p}{a}\right)^2}, \tag{12}$$

$I_\beta(z)$ and $K_\beta(z)$ are the modified Bessel functions of the first and second kind, and $C_1, \ldots, C_4$ are unknown functions of p. The pairs of functions (C_1, C_2) or (C_3, C_4) are to be determined from the boundary conditions at $x = 0$ and $x = l$. At $x = 0$ the condition is

$$\sigma_{xx}(0, t) = 0, \quad t > 0, \quad (\text{“free” boundary}) \tag{13a}$$

or

$$u(0, t) = 0, \quad t > 0, \quad (\text{“fixed” boundary}). \tag{13b}$$

At $x = l$ the slab is subjected to a stress pulse given by

$$\sigma_{xx}(l, t) = \sigma_o f(T), \qquad T = c_o t/l, \qquad t > 0, \tag{14}$$

where the constant σ_o is the magnitude of the pulse, the function f describes its time profile, and without any loss in generality, it is assumed that if $|f| \leqslant 1$. In the transform domain the boundary conditions (13) and (14) may be expressed as

$$E' \frac{\mathrm{d}}{\mathrm{d}X} \hat{U}(0, p) = 0, (\text{“free” boundary}), \tag{15a}$$

$$\hat{U}(0, p) = 0, (\text{“fixed” boundary}), \tag{15b}$$

$$E' \frac{\mathrm{d}}{\mathrm{d}X} \hat{U}(1, p) = \sigma_o \hat{f}(p), \qquad \hat{f}(p) = \int_0^\infty f(T) \mathrm{e}^{-pT} \, \mathrm{d}T. \tag{16}$$

3. SOLUTION FOR THE SLAB WITH FREE/FREE BOUNDARIES

3.1. THE CASE OF $m = n + 2$

Referring to equation (1), if $m = n + 2$ and the boundaries of the slab are free, the solution is given by equation (11b) where the functions $C_3(p)$ and $C_4(p)$ are determined from equation (15a) and (16). Thus, in the transform domain the displacement and stress may be expressed as

$$\hat{U}(X, p) = \frac{\sigma_o \hat{f}(p)}{E'_o (a+1)^{n+2} a s_3 s_4} \left[\frac{s_4 (aX+1)^{s_3} - s_3 (aX+1)^{s_4}}{(a+1)^{s_3 - 1} - (a+1)^{s_4 - 1}} \right], \tag{17}$$

$$\frac{\hat{\sigma}_{xx}(X, p)}{\sigma_0} = \hat{f}(p) \left(\frac{aX+1}{a+1} \right)^{\frac{n+1}{2}} \left\{ \frac{\mathrm{e}^{-\delta[\ln(a+1) - \ln(aX+1)]} - \mathrm{e}^{-\delta[\ln(a+1) + \ln(aX+1)]}}{1 - \mathrm{e}^{-2\delta \ln(a+1)}} \right\}, \tag{18}$$

$$\delta = \sqrt{\left(\frac{n+1}{2}\right)^2 + \left(\frac{p}{a}\right)^2}. \tag{19}$$

From a viewpoint of failure mechanics there is a greater interest in the evaluation of stresses than the displacements. The inversion of transforms such as equation (18) may be accomplished by a technique of either residue summation or wave summation. The residue summation is best suited to study the long time response, whereas the wave summation technique is more appropriate to short time analysis and is more descriptive in displaying the wave character of the response. In this study the main interest is in the transient response of the medium and, hence, only the wave solution will be developed. To do this one first expands equation (18) into an infinite series as follows:

$$\frac{\hat{\sigma}_{xx}(X,p)}{\sigma_o} = \hat{f}(p)\left(\frac{aX+1}{a+1}\right)^{\frac{n+1}{2}} \times \sum_{k=0}^{\infty}\{e^{-\delta|(2k+1)\ln(a+1)-\ln(aX+1)|} - e^{-\delta|(2k+1)\ln(a+1)+\ln(aX+1)|}\}. \tag{20}$$

Referring to the Abel–Tauber theorems regarding the asymptotic results, it is observed that for a given transform pair $g(T)$ and $\hat{g}(p)$ the asymptotic behavior of $\hat{g}(p)$ for large values of p corresponds to the behavior of $g(T)$ for small values of T. Thus, the inversion of equation (20) suitable for evaluating the small time response may be expressed as

$$\frac{\sigma_{xx}(X,T)}{\sigma_o} = \left(\frac{aX+1}{a+1}\right)^{\frac{n+1}{2}} \times \sum_{k=0}^{\infty}\left\{\left[f(T-b_{1k}) + \sum_{j=1}^{\infty}\int_0^{T-b_{1k}} f(T-b_{1k}-\tau)\frac{\alpha_{1kj}\tau^{j-1}}{(j-1)!}\,d\tau\right]H(T-b_{1k}) - \left[f(T-b_{2k}) + \sum_{j=1}^{\infty}\int_0^{T-b_{2k}} f(T-b_{2k}-\tau)\frac{\alpha_{2kj}\tau^{j-1}}{(j-1)!}\,d\tau\right]H(T-b_{2k})\right\}, \tag{21}$$

$$b_{1k} = \frac{1}{a}[(2k+1)\ln(a+1) - \ln(aX+1)],$$
$$b_{2k} = \frac{1}{a}[(2k+1)\ln(a+1) + \ln(aX+1)], \tag{22}$$

α_{1kj} and α_{2kj} are known functions of X (see Appendix A), and $H(t)$ is the Heaviside function. In the asymptotic expansions, if only the first terms are kept, the following approximation is obtained that is valid for small values of T only:

$$\frac{\sigma_{xx}(X,T)}{\sigma_o} \cong \left(\frac{aX+1}{a+1}\right)^{\frac{n+1}{2}} \sum_{k=0}^{\infty} [f(T-b_{1k})\mathrm{H}(T-b_{1k}) - f(T-b_{2k})\mathrm{H}(T-b_{2k})]. \tag{23}$$

The solution given by equation (21) can further be simplified by using the following result [23] in equation (20):

$$\frac{1}{2\pi \mathrm{i}} \int_{c-\mathrm{i}\infty}^{c+\mathrm{i}\infty} [\mathrm{e}^{-c_1 p} - \mathrm{e}^{-c_1\sqrt{p^2+c_2^2}}]\mathrm{e}^{pt}\,\mathrm{d}p = 0, \qquad 0 < t < c_1,$$
$$= \frac{c_1 c_2 \mathrm{J}_1(c_2\sqrt{t^2-c_1^2})}{\sqrt{t^2-c_1^2}}, \qquad t > c_1, \tag{24}$$

where $\mathrm{Re}(p) > |\mathrm{Im}(c_2)|$ and $\mathrm{J}_1(z)$ is the Bessel function of the first kind of order one. From equations (20) and (24) it may then be shown that

$$\frac{\sigma_{xx}(X,T)}{\sigma_o} = \left(\frac{aX+1}{a+1}\right)^{\frac{n+1}{2}} \times \sum_{k=0}^{\infty} \left\{ \left[f(T-b_{1k}) - \int_0^{\sqrt{T^2-b_{1k}^2}} f(T-\sqrt{\tau^2+b_{1k}^2}) \frac{(n+1)ab_{1k}\mathrm{J}_1\left(\frac{n+1}{2}a\tau\right)}{2\sqrt{\tau^2+b_{1k}^2}}\,\mathrm{d}\tau \right] \right.$$
$$\times \mathrm{H}(T-b_{1k}) - \left[f(T-b_{2k}) - \int_0^{\sqrt{T^2-b_{2k}^2}} f(T-\sqrt{\tau^2+b_{2k}^2}) \right.$$
$$\left. \left. \times \frac{(n+1)ab_{2k}\mathrm{J}_1\left(\frac{n+1}{2}a\tau\right)}{2\sqrt{\tau^2+b_{2k}^2}}\,\mathrm{d}\tau \right] \mathrm{H}(T-b_{2k}) \right\}, \tag{25}$$

where b_{1k} and b_{2k} are again given by equation (22). The solution given by equation (25) is "exact" and can be used to assess the effectiveness of the asymptotic techniques by, for example, comparing the results obtained from equations (21) and (25).

3.2. THE CASE OF $m \neq n+2$

In the material model described by equation (1), if $m \neq n+2$, then the solution is given by equation (11a) with equations (15a) and (16) to be used to determine $C_1(p)$ and $C_2(p)$. The transform of the stress may then be expressed as

$$\frac{\hat{\sigma}_{xx}(X,p)}{\sigma_o} = \hat{f}(p)\left(\frac{aX+1}{a+1}\right)^{\frac{m+n}{4}}\left[\frac{W_{1x}e^{(z_o-z_x)} - W_{2x}e^{-(z_o-z_x)}}{W_{1l}e^{(z_o-z_l)} - W_{2l}e^{-(z_o-z_l)}}\right],$$
$$z_x = \left|\frac{2p}{(n-m+2)a}\right|(aX+1)^{\frac{n-m+2}{2}}, \qquad z_o = \left|\frac{2p}{(n-m+2)a}\right|, \tag{26}$$

$$z_l = \left|\frac{2p}{(n-m+2)a}\right|(a+1)^{\frac{n-m+2}{2}}. \tag{27}$$

The functions W_{1x}, W_{2x}, W_{1l}, and W_{2l} are given in Appendix B. To perform the asymptotic analysis first one observes that for large $|z|$ one has [24]

$$\frac{\sqrt{2\pi z}}{e^z}I_\nu(z) = \sum_{k=0}^{\infty}\frac{(\nu,k)}{(-2z)^k} + e^{-2z-(\nu+\frac{1}{2})\pi i}\sum_{k=0}^{\infty}\frac{(\nu,k)}{(2z)^k}, \qquad -\frac{3}{2}\pi < \arg z < \frac{1}{2}\pi,$$
$$= \sum_{k=0}^{\infty}\frac{(\nu,k)}{(-2z)^k} + e^{-2z+(\nu+\frac{1}{2})\pi i}\sum_{k=0}^{\infty}\frac{(\nu,k)}{(2z)^k}, \qquad -\frac{1}{2}\pi < \arg z < \frac{3}{2}\pi, \tag{28}$$

$$\sqrt{\frac{2z}{\pi}}e^z K_\nu(z) = \sum_{k=0}^{\infty}\frac{(\nu,k)}{(2z)^k}, \tag{29}$$

where (ν, k) is the Hankel symbol defined by

$$(\nu,k) = 1, k = 0,$$
$$= \frac{\Gamma\left(\nu+\frac{1}{2}+k\right)}{k!\Gamma\left(\nu+\frac{1}{2}-k\right)} = \frac{2^{-2k}}{k!}\{(4\nu^2-1^2)(4\nu^2-3^2)\ldots[4\nu^2-(2k-1)^2]\},$$
$$k > 0. \tag{30}$$

By substituting from equations (28), (29), and Appendix B into equation (26), arranging the expansion to a suitable form for wave summation and inverting the result, one obtains an asymptotic solution similar to equation (21). For example, it may be observed that for large values of p the first term approximations are

$$W_{1x} \cong W_{2x} \cong W_{1l} \cong W_{2l} \cong 4, \tag{31}$$

giving an asymptotic result for $\sigma_{xx}(X, T)$ as follows:

$$\frac{\delta_{xx}(X,T)}{\sigma_o} \cong \left(\frac{aX+1}{a+1}\right)^{\frac{m+n}{4}}\sum_{k=0}^{\infty}[f(T-\zeta_{1k})H(T-\zeta_{1k}) - f(T-\zeta_{2k})H(T-\zeta_{2k})], \tag{32}$$

where the functions ζ_{1k} and ζ_{2k} are given by

$$\zeta_{1k} = \left|\frac{2}{(n-m+2)a}\right|\left|(2k+1)(a+1)^{\frac{n-m+2}{2}} - 2k - (aX+1)^{\frac{n-m+2}{2}}\right|,$$
$$\zeta_{2k} = \left|\frac{2}{(n-m+2)a}\right|\left|(2k+1)(a+1)^{\frac{n-m+2}{2}} - (2k+2) + (aX+1)^{\frac{n-m+2}{2}}\right|. \tag{33}$$

4. THE SOLUTION FOR FIXED/FREE BOUNDARIES

4.1. THE CASE OF $m = n+2$

In this case the solution in the transform domain is given by equation (11b) subject to boundary conditions (15b) and (16). Thus, after determining C_3 and C_4, $\hat{\sigma}_{xx}$ may be expressed as

$$\frac{\hat{\sigma}_{xx}(X,p)}{\sigma_o} = \hat{f}(p)\left(\frac{aX+1}{a+1}\right)^{\frac{n+1}{2}}\sum_{k=0}^{\infty}(-1)^k\left\{\left(\frac{2\delta+n+1}{2\delta-n-1}\right)^k \mathrm{e}^{-\delta[(2k+1)\ln(a+1)-\ln(aX+1)]}\right.$$
$$\left.+\left(\frac{2\delta+n+1}{2\delta-n-1}\right)^{k+1}\mathrm{e}^{-\delta[(2k+1)\ln(a+1)+\ln(aX+1)]}\right\} \tag{34a}$$

for $n \leqslant -1$ and $a > 0$, or $(n+1)\ln(a+1) < 4$, and

$$\frac{\hat{\sigma}_{xx}(X,p)}{\sigma_o} = \hat{f}(p)\left(\frac{aX+1}{a+1}\right)^{\frac{n+1}{2}}\sum_{k=0}^{\infty}(-1)^k\left\{\left(\frac{2\delta-n-1}{2\delta+n+1}\right)^{k+1} \mathrm{e}^{\delta[(2k+1)\cdot\ln(a+1)+\ln(aX+1)]}\right.$$
$$\left.+\left(\frac{2\delta-n-1}{2\delta+n+1}\right)^{k}\mathrm{e}^{\delta[(2k+1)\cdot\ln(a+1)-\ln(aX+1)]}\right\} \tag{34b}$$

for $n > -1$ and $-1 < a < 0$. In equation (34) δ is defined by equation (19). Note that the transforms given by equation (34) are quite similar to equation (20) and would lead to an asymptotic solution in the wave summation form similar to equation (21). Also note that for large values of p one has a first term approximation

$$\frac{2\delta+n+1}{2\delta-n-1} \cong \frac{2\delta-n-1}{2\delta+n+1} \cong 1, \tag{35}$$

giving the following asymptotic expression for σ_{xx}:

$$\frac{\sigma_{xx}(X,T)}{\sigma_o} \cong \left(\frac{aX+1}{a+1}\right)^{\frac{n+1}{2}}\sum_{k=0}^{\infty}(-1)^k[f(T-b_{1k})\mathrm{H}(T-b_{1k}) + f(T-b_{2k})\mathrm{H}(T-b_{2k})], \tag{36}$$

where b_{1k} and b_{2k} are given by equation (22).

4.2. THE CASE OF $m \neq n+2$

In this problem the solution is given by equations (11a), (15b), and (16), and the transform of the stress may be expressed as

$$\frac{\hat{\sigma}_{xx}(X,p)}{\sigma_o} = \hat{f}(p)\left(\frac{aX+1}{a+1}\right)^{\frac{m+n}{4}}\left[\frac{W_{3x}e^{(z_o-z_x)} + W_{4x}e^{-(z_o-z_x)}}{W_{3l}e^{(z_o-z_l)} + W_{4l}e^{-(z_o-z_l)}}\right], \tag{37}$$

where the functions z_x, z_o, and z_l are defined by equation (27) and W_{3x}, W_{4x}, W_{3l}, and W_{4l} are given in Appendix B. Again, it is observed that equation (37) is quite similar to equation (26) and would lead to a similar asymptotic solution suitable for evaluating the response for small T. Also, for large values of p one has

$$W_{3x} \cong W_{4x} \cong W_{3l} \cong W_{4l} \cong 2, \tag{38}$$

giving the first term asymptotic expression for the stress as follows:

$$\frac{\sigma_{xx}(X,T)}{\sigma_o} \cong \left(\frac{aX+1}{a+1}\right)^{\frac{m+n}{4}}\sum_{k=0}^{\infty}(-1)^k[f(T-\zeta_{1k})\mathrm{H}(T-\zeta_{1k}) + f(T-\zeta_{2k})\mathrm{H}(T-\zeta_{2k})], \tag{39}$$

where ζ_{1k} and ζ_{2k} are given by equation (33).

5. RESULTS AND DISCUSSION

As a first example we consider an FGM slab that consists of nickel and zirconia. We assume that the thickness of the plate is $l = 5$ mm, on one surface the medium is pure nickel, on the other surface pure zirconia, and the material properties $E'(x)$ and $\rho(x)$ vary smoothly in thickness direction. A pressure pulse defined by

$$\sigma_{xx}(l,t) = \sigma_o f(t) = -\sigma_o[\mathrm{H}(t) - \mathrm{H}(t-t_o)] \tag{40}$$

is applied to the surface $x = l$ and the boundary $x = 0$ is either "free" or "fixed" (Figure 1). The pulse duration is assumed to be $t_o = 0{\cdot}2$ μs. The properties of the constituent materials used in the examples are given in Table 1. Referring to the boundary conditions and material compositions shown in Figures 1 and 2, respectively, it is seen that there are four different numerical problems.

The material parameters defined by equations (1) and (2) for the FGMs used in the examples are given in Table 2. To examine the accuracy of the asymptotic results given in sections 3 and 4, we consider the Ni/ZrO_2 slab with free/free boundaries subjected to the pulse given by equation (40) on the ZrO_2 side (Figures 1(a) and 2(a)). The exact solution of the problem is given by equation (25) whereas equation (21) gives the asymptotic result. The accuracy of the result would be expected to depend on the number of terms retained in the inner series in equation (21). For the example considered Table 3 shows the comparison of the normalized stress σ_{xx}/σ_o obtained from the exact solution (25) and from equation (21) by retaining a limited number of terms in the inner series. The

TABLE 1
Properties of materials used in the examples

	E (GPa)	ν	ρ (kg/m^3)
ZrO_2	151	0·33	5331
Ni	207	0·31	8900
SiC	210	0·17	3100
Al	71	0·33	2710

results are given at three locations in the slab for five different values of time. It may be seen that the convergence is quite good and by retaining, for example, six terms, the accuracy of the results is five significant digits or better. In the calculated results for σ_{xx}/σ_o given in this section, equation (21) and (the inversion of) equation (34) are used by retaining six terms in the asymptotic expansion. The stress is calculated up to 12 μs (the propagation time of the plane wave through the thickness $l = 5$ mm is approximately 0·77 μs in pure ZrO_2 and 0·88 μs in Ni). However, it is clear that if the response is required for larger values of time, one may need to use a greater number of terms in the asymptotic expansion and a convergence check may have to be performed.

For various combinations of boundary conditions and material compositions shown in Figures 1 and 2 the normalized stress is given in Figures 3–15. Figures 3 and 9 show a sketch describing the variation of σ_{xx}/σ_o with x and t. In all cases the initial pulse is applied at $x = l$. If the conditions shown in Figures 1(a), (b) and 2(a), (b) are designated as (a, b) and (a, b), respectively, the groups of Figures 3–6, 7–8, 9–12, and 13–15 correspond to the conditions aa, ab, ba, and bb, respectively. For example, Figure 4 shows the stress as a function of location x for three different values of time and Figures 5 and 6 show the time dependence of the stress at locations $x/l = 1/50$ and $x/l = 1/2$, respectively, for boundary conditions described by Figure 1(a)and material composition given by

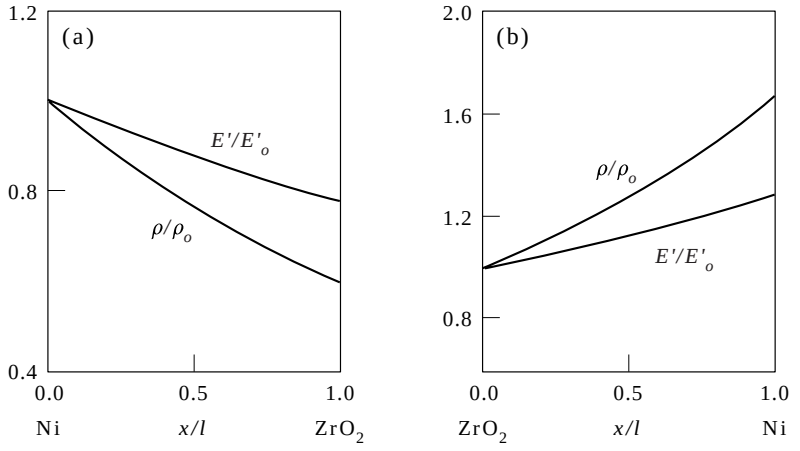

Figure 2. The variation of density and elastic modulus in (a) Ni/ZrO_2 and (b) ZrO_2/Ni FGM slabs (Table 2 and equation(l)).

TABLE 2

Material constants of FGMs used in the examples and defined by equations (1) *and* (2)

	Ni/ZrO_2 (Figure 2(a))	ZrO_2/Nr (Figure 2(b))	SiC/Al (Figure 18(a))	Al/SiC (Figure 18(b))
E_o' (GPa)	286·922	223·728	225·719	105·197
ρ_o (kg/m^3)	8900	5331	3100	2710
a	−0·14096	−0·12354	−0·53395	1·14568
m	−1·8866	−1·8866	1·00000	1·0000
n	−3·8866	−3·8866	0·17611	0·17611

TABLE 3

Normalized stress $\sigma_{xx}(x, t)/\sigma_o$ *obtained from the exact solution and asymptotic approximation for* Ni/ZrO_2 *FGM slab with free/free boundaries subjected to a rectangular pulse on the* ZrO_2 *side* (*Figures* 1(a) *and* 2(a))

	$t(\mu s)$	$x/l = 0·2$	$x/l = 0·5$	$x/l = 0·8$
Exact solution	2	−0·0021322348	−0·0049332263	−1·0343400828
	4	−1·1595629726	0·0117491390	0·0043553632
	6	1·1790003476	0·0160863639	0·0059628547
	8	−0·0111121299	1·0798490653	0·0073659788
	10	−0·0128308112	−0·296942924	−0·0441531228
1-term approximation	2	0	0	−1·0367694771
	4	−1.1620637970	0	0
	6	1·1620637970	0	0
	8	0	1·0963939785	0
	10	0	0	0
2-term approximation	2	−0.0021544500	−0.0049795629	−1.0343718842
	4	−1·1596961101	0·0116548623	0·0043244623
	6	1·1793189959	0·0163168071	0·0060542473
	8	−0·0107722501	1·0806462086	0·0077840322
	10	−0·0129267001	−0·0298773776	−0·0443243692
3-term approximation	2	−0·0021238545	−0·0049188718	−1·0343310106
	4	−1·1595538472	0·0117659643	0·0043688333
	6	1·1790142310	0·0161143887	0·0059847764
	8	−0·0110795420	1·0799049378	0·0074029926
	10	−0·0127907636	−0·0296233326	−0·0441039430
6-term approximation	2	−0·0021322342	−0·0049332252	−1·0343400822
	4	−1·1595629633	0·0117491541	0·0043553716
	6	1·1790003831	0·0160864208	0·0059628866
	8	−0·0111120446	1·0798492024	0·0073660561
	10	−0·0128306451	−0·0296940260	−0·0441529725
8-term approximation	2	−0·0021322348	−0·0049332263	−1·0343400828
	4	−1·1595629729	0·0117491386	0·0043553628
	6	1·1790003456	0·0160863608	0·0059628528
	8	−0·0111121395	1·0798490502	0·0073659703
	10	−0·0128308411	−0·0296943400	−0·0441531497

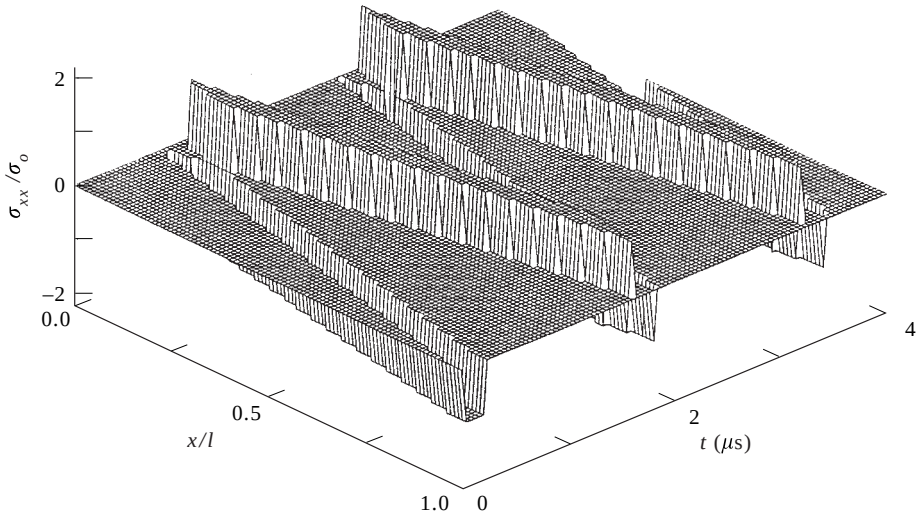

Figure 3. The variation of normalized stress with x and t, the case aa (Figures 1(a), 2(a), $l = 5$ mm, $t_o = 0{\cdot}2$ μs).

Figure 2(a), or for the case aa. Note that at $x = 0$ the stress is zero and $x = l/50$ was selected to have some idea about the spallation stress near the boundary. The results for $x = l/2$ are given to provide a typical stress/time profile for various conditions considered.

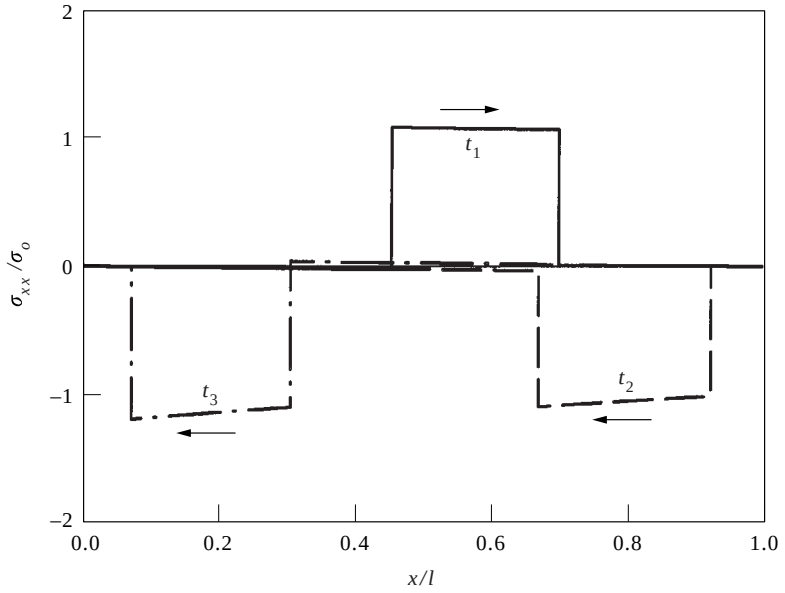

Figure 4. The variation of normalized stress with x at $t_1 = 8$ μs, $t_2 = 8{\cdot}5$ μs, and $t_3 = 9$ μs, the case aa; the arrows indicate the direction of pulse propagation (Figures 1(a), 2(a), $l = 5$ mm, $t_o = 0{\cdot}2$ μs).

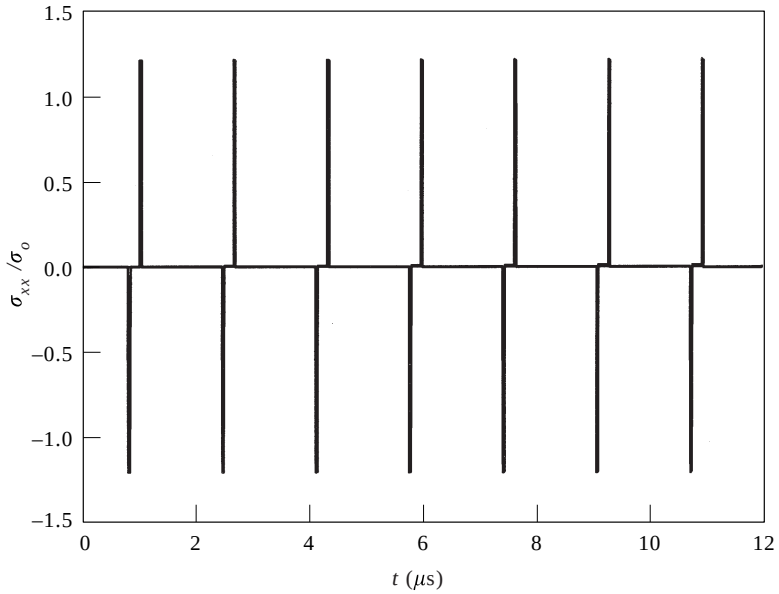

Figure 5. The variation of σ_{xx}/σ_o with t at a fixed location $x = l/50$, the case aa (Figures 1(a), 2(a), $l = 5$ mm, $t_o = 0{\cdot}2$ μs).

By examining the results given in Figures 4–6, where the boundaries of the slab are stress-free and the pulse is applied on the less stiff side (condition aa), it may be observed that the duration of the pulse remains constant (at $\Delta t = t_0 = 0{\cdot}2$ μs), the pulse shape is distorted as time increases, at a given location the jump $\Delta\sigma$ in stress corresponding to leading and trailing edges of the pulse

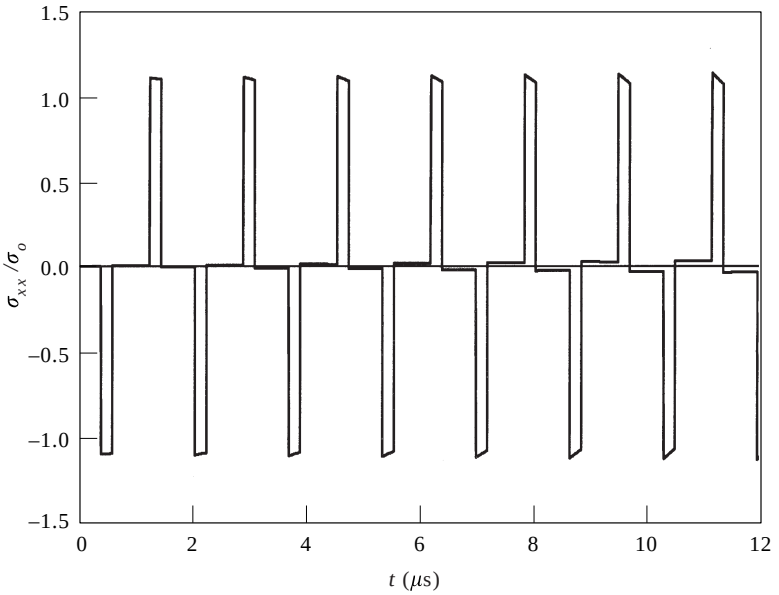

Figure 6. The variation of σ_{xx}/σ_o with t at a fixed location $x = l/2$, the case aa (Figures 1(a), 2(a), $l = 5$ mm, $t_o = 0{\cdot}2$ μs).

remains constant but its value is dependent on the location x, at $x=l$, $\Delta\sigma=\sigma_o$, for $0<x<l$, $\Delta\sigma>\sigma_o$, and as x decreases, $\Delta\sigma$ increases slightly but monotonically. After the pulse passes through the stress does not drop to zero and this overshoot seems to increase with time. Similar observations may be made for condition ab shown in Figures 7 and 8. In this case too, $\Delta\sigma=\sigma_o$ at $x=l$, but it decreases monotonically with decreasing x (or decreasing stiffness). These deviations from the homogeneous materials (shown for reference in a pure nickel slab by Figures 16 and 17) are much more pronounced in the case of fixed/free boundaries (ba and bb) than for free/free boundaries (aa and ab). This can be clearly seen from Figures 9–15. As shown by Figures 11 and 14 there is the standard doubling of the amplitude of the pulse reflected from the fixed boundary at $x=0$. However, as in the case of free/free boundaries (Figure 5), in this case, too, if the fixed boundary $x=0$ is the stiffer side of FGM, then the jump $2\Delta\sigma$ in the reflected pulse is greater than $2\sigma_o$ (Figure 11, case ba) and if $x=0$ is the less stiff side, then $2\Delta\sigma<2\sigma_o$ (Figure 14, case bb). Again, the jump discontinuity $\Delta\sigma$ in stress is a function in x but at a given location x it is independent of t. $\Delta\sigma=\sigma_o$ at $x=l$, and increases monotonically as the stiffness of the medium increases (Figure 10, case ba) or decreases as the stiffness decreases (Figure 13, case bb). One may also observe that in the case of fixed/free boundaries (ba and bb), the magnitude of the overshoot is no longer small compared to σ_o. Since at a given location $\Delta\sigma$ is constant, this could be an additional source of stress amplification.

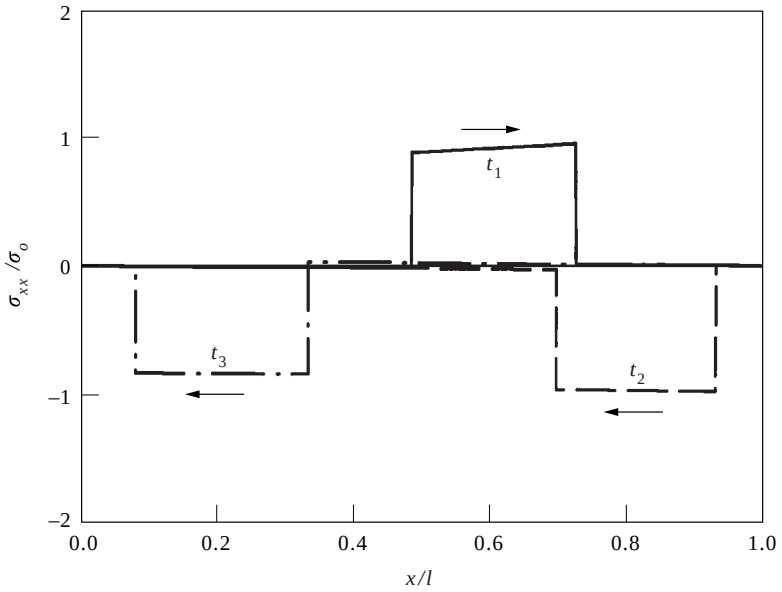

Figure 7. The variation of σ_{xx}/σ_o with x at $t_1=8$ μs, $t_2=8{\cdot}5$ μs, and $t_3=9$ μs, the case ab; the arrows indicate the direction of pulse propagation (Figures 1(a), 2(b), $l=5$ mm, $t_o=0{\cdot}2$ μs).

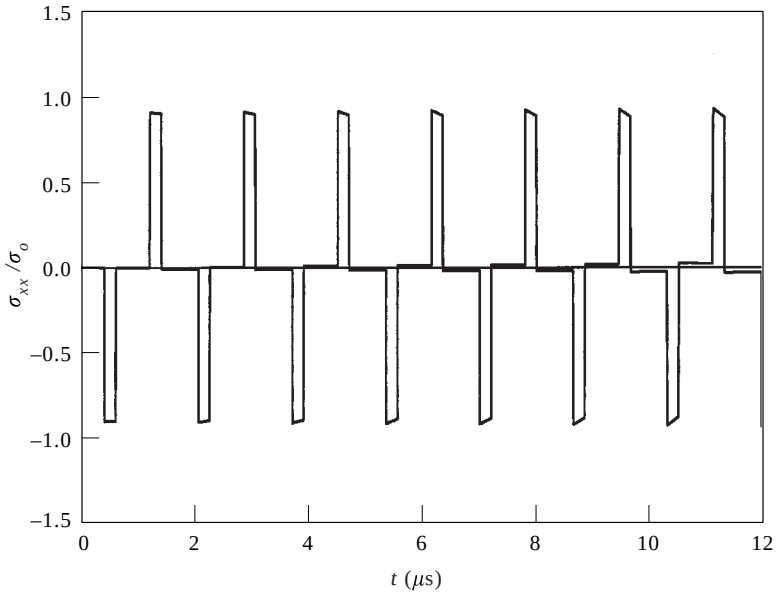

Figure 8. The variation of σ_{xx}/σ_o with t at $x = l/2$, the case ab (Figures 1(a), 2(b), $l = 5$ mm, $t_o = 0{\cdot}2$ μs).

Most of the observations made in this section may be verified by examining the asymptotic results given in sections 3 and 4, in particular the one-term approximations expressed by equations (23), (32), (36), and (39) for various cases. The fact that the pulse duration $\Delta t = t_o$ is constant may be seen from equation (40) and one term asymptotic expressions. The wave summation

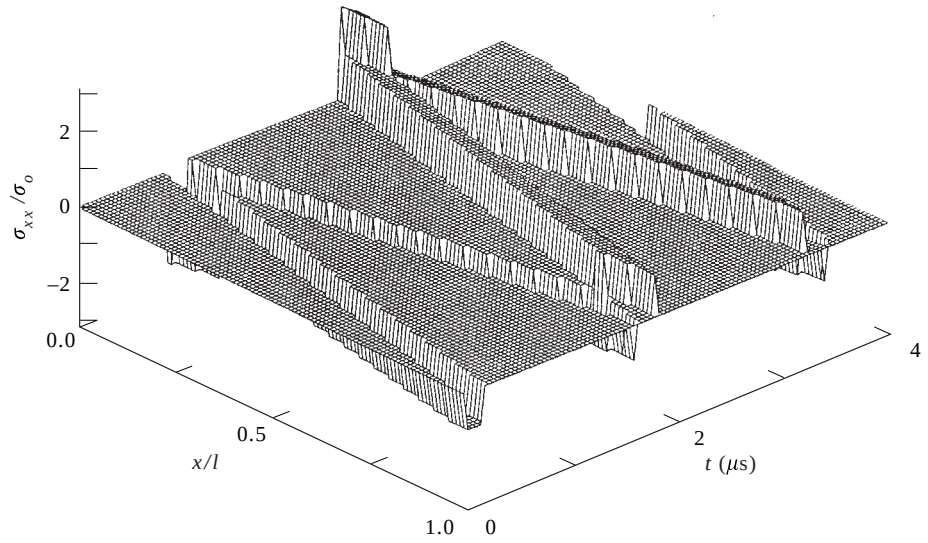

Figure 9. The variation of σ_{xx}/σ_o with x and t, the case ba (Figures 1(b), 2(a), $l = 5$ mm, $t_o = 0{\cdot}2$ μs).

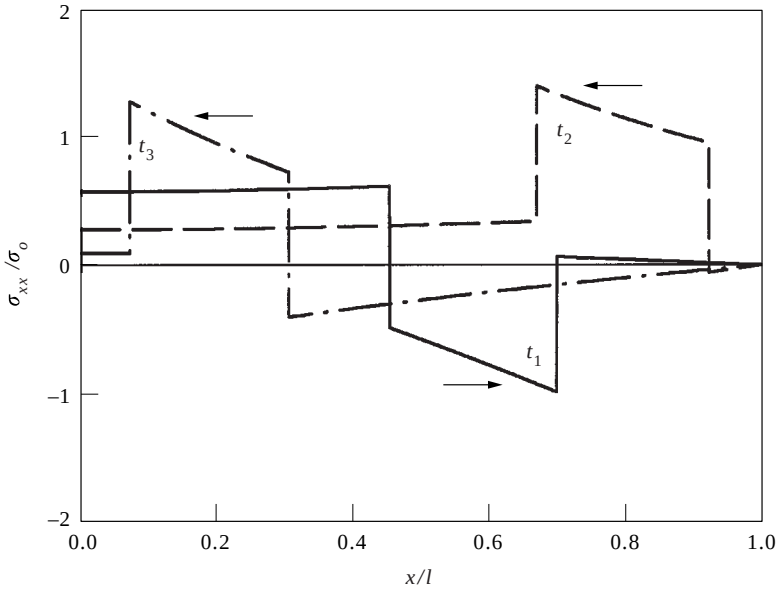

Figure 10. The variation of σ_{xx}/σ_o with x at $t_1 = 8$ μs, $t_2 = 8{\cdot}5$ μs, and $t_3 = 9$ μs, the case ba; the arrows indicate the direction of pulse propagation (Figures 1(b), 2(a), $l = 5$ mm, $t_o = 0{\cdot}2$ μs).

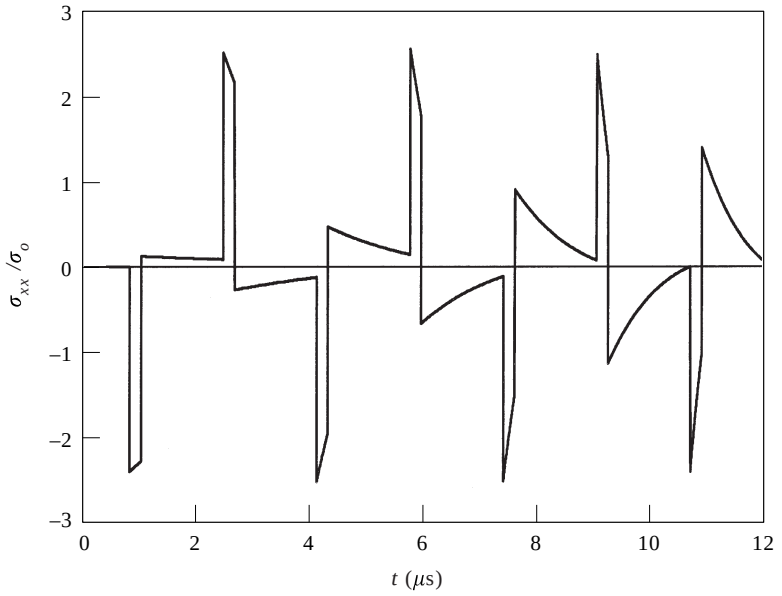

Figure 11. The variation of σ_{xx}/σ_o with t at $x = 0$, the case ba (Figures 1(b), 2(a), $l = 5$ mm, $t_o = 0{\cdot}2$ μs).

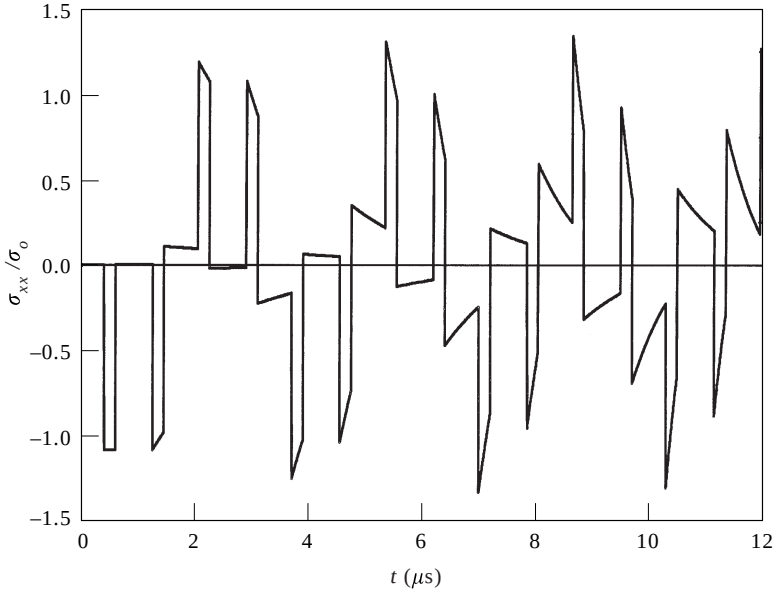

Figure 12. The variation of σ_{xx}/σ_o with t at $x = l/2$, the case ba (Figures 1(b), 2(a), $l = 5$ mm, $t_o = 0{\cdot}2$ μs).

aspects of the solutions representing the interactions of waves with boundaries are similar to those in homogeneous media, except that due to material inhomogeneity the wave speeds are variable. The asymptotic results show that the magnitude of the jump discontinuity in stress may be expressed as

$$\frac{\Delta\sigma}{\sigma_o} = \psi_o(x) = \left[\frac{a(x/l)+1}{a+1}\right]^{\frac{m+n}{4}}. \tag{41}$$

From equations (41) and (1) it follows that

$$\psi_o(x) = \left[\frac{E'(x)\rho(x)}{E'(l)\rho(l)}\right]^{\frac{1}{4}}. \tag{42}$$

Thus, from equation (42) and Figure 2 it is seen that $\psi_o(l) = 1$, $\psi_o(x) > 1$ for cases aa and ba (Figure 2(a)) and $\psi_o(x) < 1$ for cases ab and bb (Figure 2(b)). Needless to say, the actual values of $(\sigma_{xx})_{max}$ will be the sum of $\Delta\sigma$ and the overshoot. The results described by the figures and Table 3 indicate that the overshoot is dependent on the boundary conditions and the material composition, and there is no simple way of estimating its magnitude. In many cases, however, the overshoot may be negligible and at a given location x the maximum stress may be approximated by

$$(\sigma_{xx}(x,t))_{max} \cong K\psi_o(x)\sigma_o, \tag{43}$$

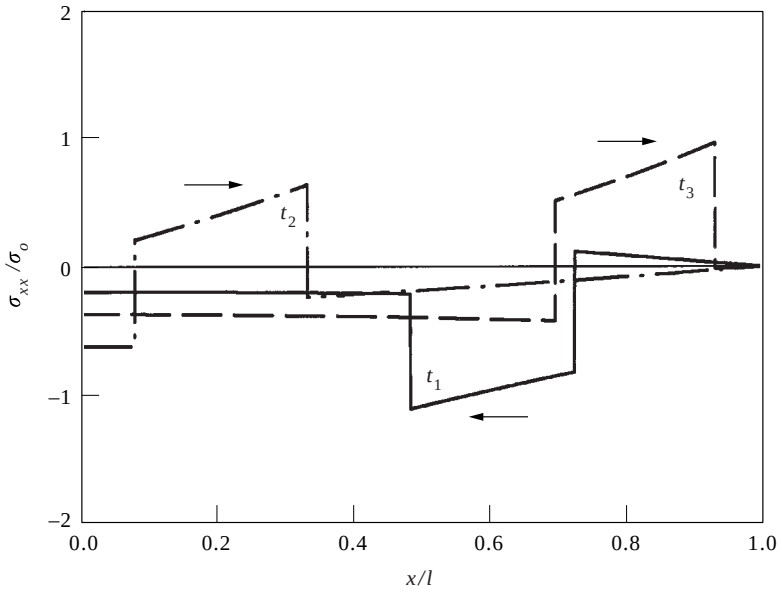

Figure 13. The variation of σ_{xx}/σ_o with x at $t_1 = 8$ μs, $t_2 = 8{\cdot}5$ μs, and $t_3 = 9$ μs, the case bb; the arrows indicate the direction of pulse propagation (Figures 1(b), 2(b), $l = 5$ mm, $t_o = 0{\cdot}2$ μs).

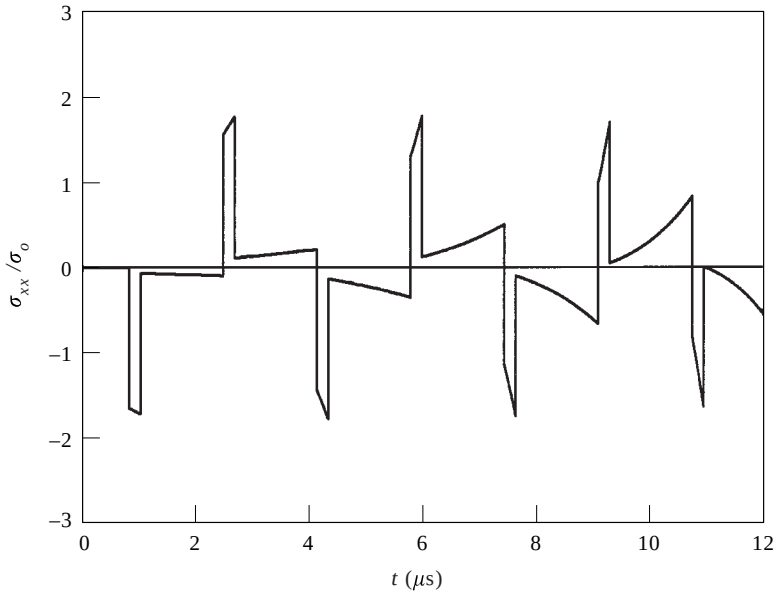

Figure 14. The variation of σ_{xx}/σ_o with t at $x = 0$, the case bb (Figures 1(b), 2(b), $l = 5$ mm, $t_o = 0{\cdot}2$ μs).

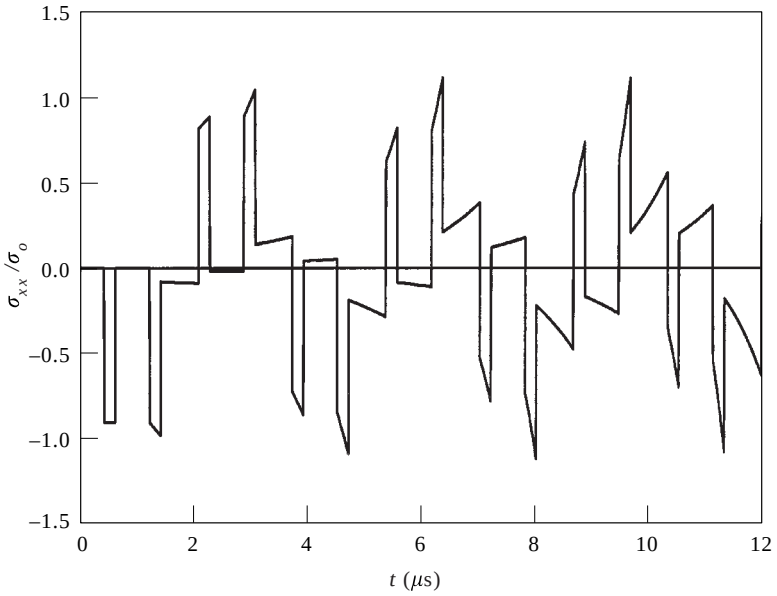

Figure 15. The variation of σ_{xx}/σ_o with t at $x = l/2$, the case bb (Figures 1(b), 2(b), $l = 5$ mm, $t_o = 0{\cdot}2$ μs).

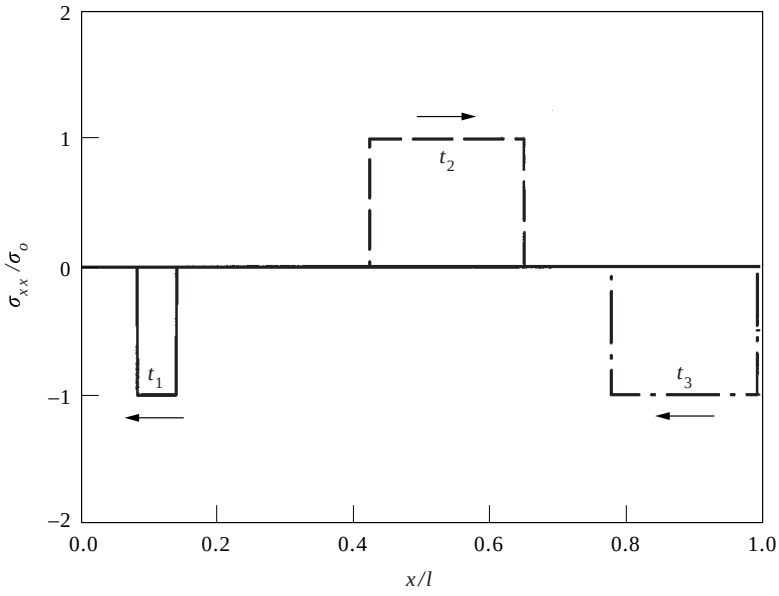

Figure 16. The variation of σ_{xx}/σ_o as a function of x at $t_1 = 8$ μs, $t_2 = 8{\cdot}5$ μs, and $t_3 = 9$ μs in a homogeneous nickel slab with free/free boundaries; the arrows indicate the direction of pulse propagation (Figure 1(a), $l = 5$ mm, $t_o = 0{\cdot}2$ μs).

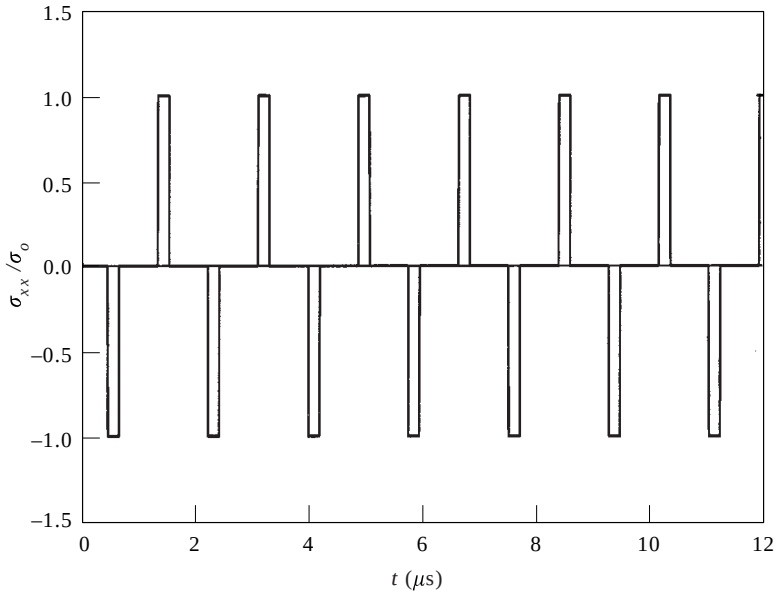

Figure 17. The variation of σ_{xx}/σ_o as a function of t at $x = l/2$ in a homogeneous nickel slab with free/free boundaries (Figure 1(a), $l = 5$ mm, $t_o = 0{\cdot}2$ μs).

where $K = 1$ for free/free and $K = 2$ for fixed/free boundaries (Figure 1). If one further assumes that the density and the Poisson's ratio are constant, then equation (42) becomes

$$\psi_o(x) = \left[\frac{E(x)}{E(l)}\right]^{\frac{1}{4}}. \tag{44}$$

This is the result found by Steele [15] from the leading term of an asymptotic solution based on geometric optics.

The simple expressions (42) and (44) giving the stress magnification factor $\psi_o(x)$ appear to be independent of the material model used. For example, instead of equation (1), if the parameters of the inhomogeneous medium are given by

$$E'(x) = E'_o e^{\alpha x}, \qquad \rho(x) = \rho_o e^{\alpha x}, \qquad c = \sqrt{E'_o/\rho_o}, \tag{45}$$

the exact and first term asymptotic expressions of the normalized stress may be obtained by following the procedure outlined in sections 2 and 3. The solution is given in Appendix C from which it is seen that

$$\frac{\Delta\sigma}{\sigma_o} = \psi_o(x) = e^{-\frac{\alpha}{2}(l-x)}. \tag{46}$$

From equations (45) and (46) one finds

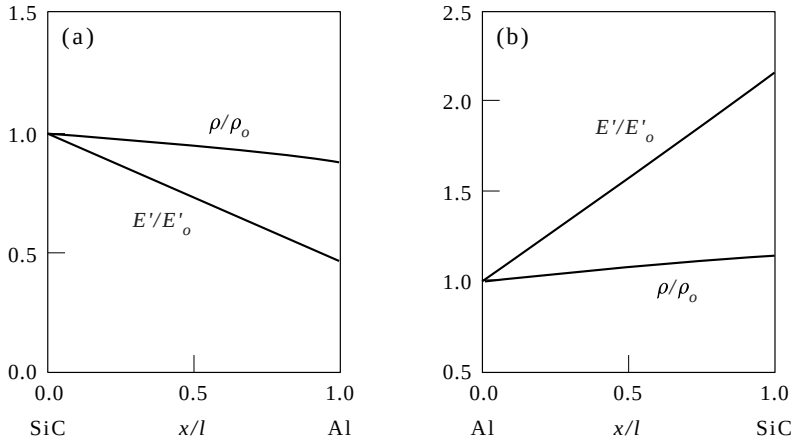

Figure 18. The variation of elastic modulus and density in (a) SiC/Al and (b) Al/SiC FGM slabs (Table 2 and equation (1)).

$$\psi_o(x) = \left[\frac{\rho(x)}{\rho(l)}\right]^{\frac{1}{2}} = \left[\frac{E'(x)}{E'(l)}\right]^{\frac{1}{2}}, \tag{47}$$

which is a special case of equation (42).

As a second example, consider the pulse propagation in an FGM slab that consists of aluminum and silicon carbide described in Figure 18. Referring to

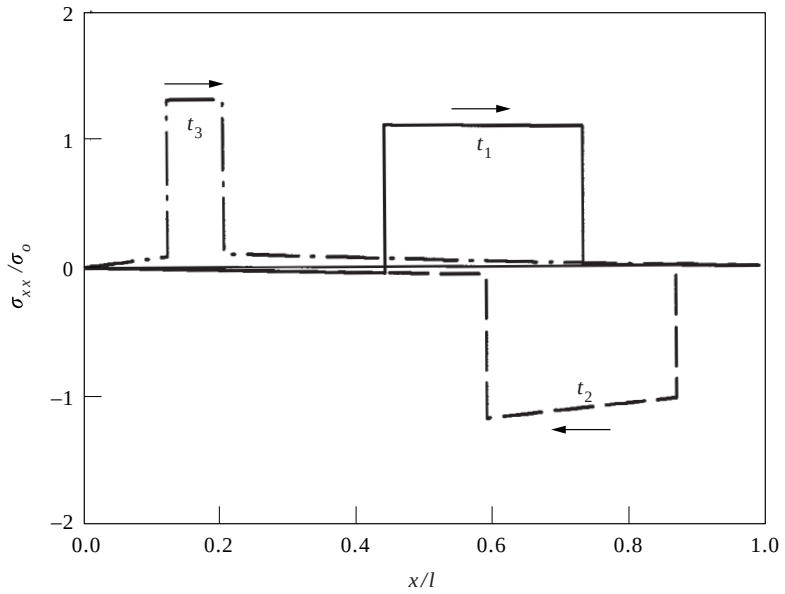

Figure 19. The variation of normalized stress with x in a SiC/Al FGM under free/free boundary conditions at $t_1 = 2{\cdot}5$ μs, $t_2 = 3$ μs, and $t_3 = 3{\cdot}5$ μs; the arrows indicate the direction of pulse propagation (Figures 1(a), 18(a), $l = 5$ mm, $t_o = 0{\cdot}2$ μs).

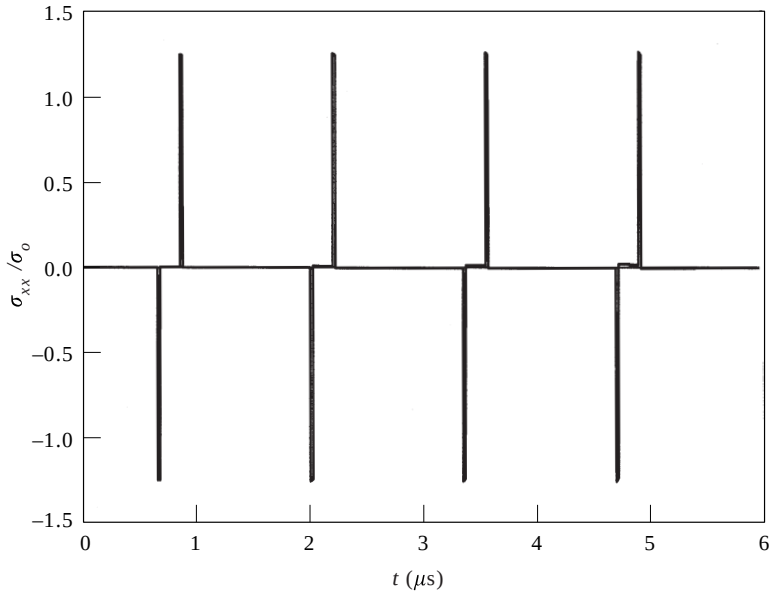

Figure 20. Variation of stress with t in a SiC/Al FGM under free/free boundary conditions at $x = l/50$ (Figures 1(a), 18(a), $l = 5$ mm, $t_o = 0{\cdot}2$ μs).

equation (1) and Table 2, it is seen that $m \neq n + 2$ and consequently the solution is somewhat more complicated. The results for free/free and fixed/free boundary conditions are given in sections 3.2 and 4.2, respectively. Again the thickness of the slab is $l = 5$ mm, the pulse duration is $t_o = 0{\cdot}2$ μs (see equation (40)), and the pulse is applied at $x = l$. For SiC/Al and Al/SiC FGMs described in Figures

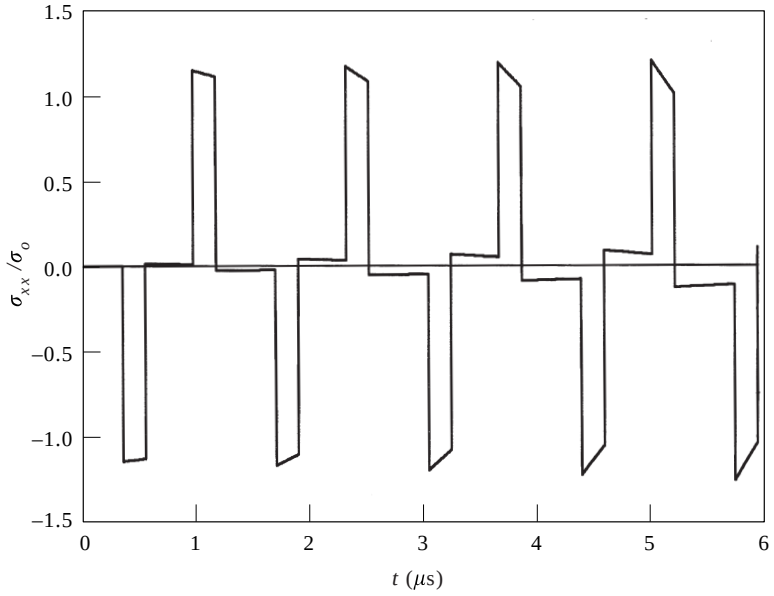

Figure 21. The variation of σ_{xx}/σ_o with t in a SiC/Al FGM under free/free boundary conditions at $x = l/2$ (Figures 1(a), 18(a), $l = 5$ mm, $t_o = 0{\cdot}2$ μs).

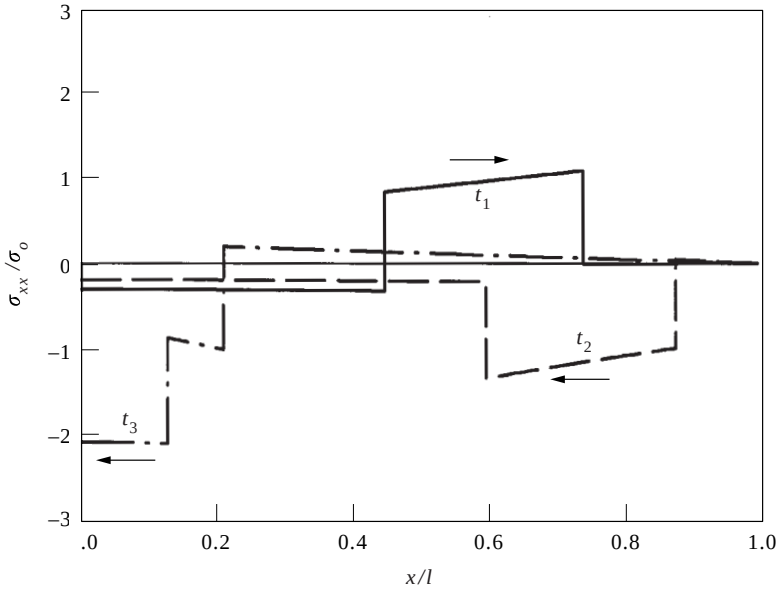

Figure 22. The variation of σ_{xx}/σ_o with x in a SiC/Al FGM under fixed/free boundary conditions at $t_1 = 2{\cdot}5$ μs, $t_2 = 3$ μs, and $t_3 = 3{\cdot}5$ μs; the arrows indicate the direction of pulse propagation (Figures 1(b), 18(a), $l = 5$ mm, $t_o = 0{\cdot}2$ μs).

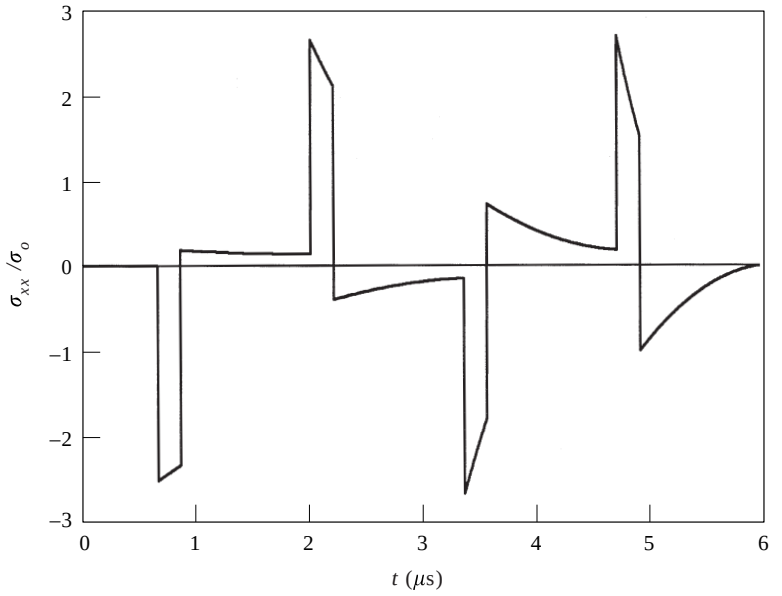

Figure 23. The variation of σ_{xx}/σ_o with t in a SiC/Al FGM under free/free boundary conditions at $x = 0$ (Figures 1(b), 18(a), $l = 5$ mm, $t_o = 0{\cdot}2$ μs).

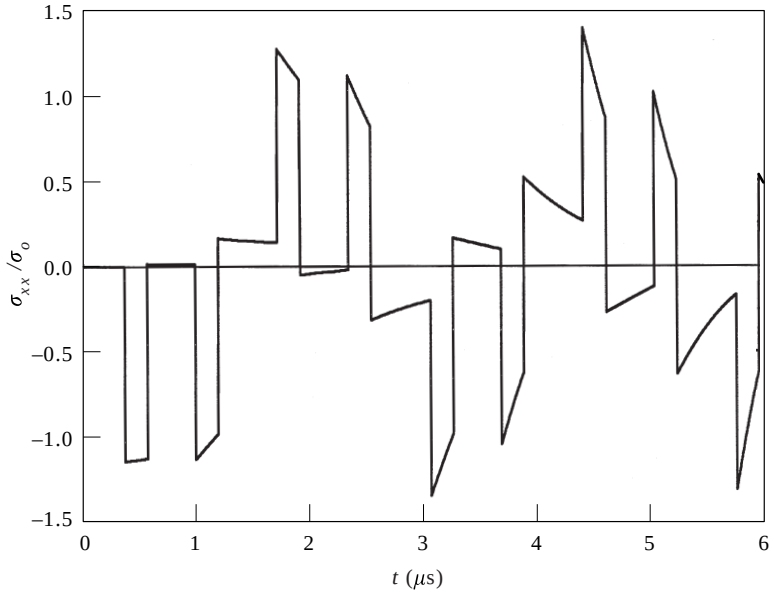

Figure 24. The variation of σ_{xx}/σ_o with t in a SiC/Al FGM under fixed/free boundary conditions at $x = l/2$ (Figures 1(b), 18(a), $l = 5$ mm, $t_o = 0{\cdot}2$ μs).

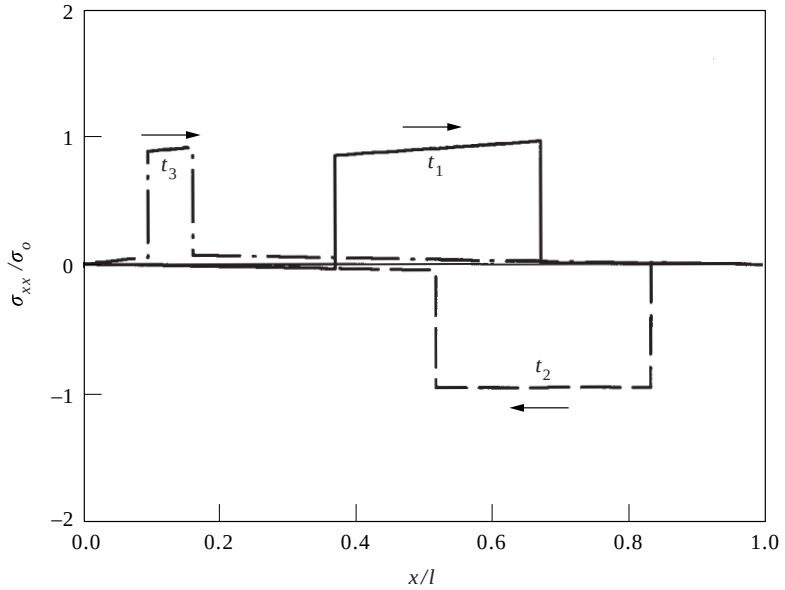

Figure 25. The variation of normalized stress with x in an Al/SiC FGM under free/free boundary conditions at $t_1 = 2{\cdot}5$ μs, $t_2 = 3$ μs, and $t_3 = 3{\cdot}5$ μs; the arrows indicate the direction of pulse propagation (Figures 1(a), 18(b), $l = 5$ mm, $t_o = 0{\cdot}2$ μs).

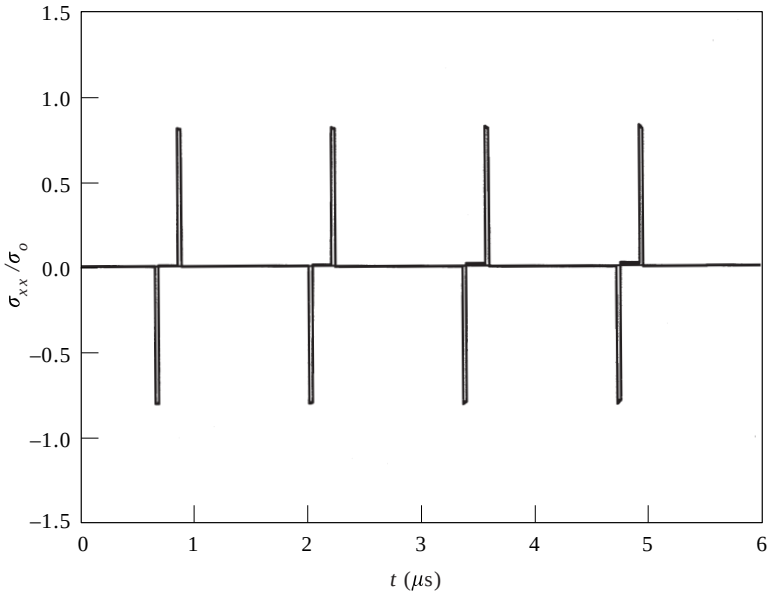

Figure 26. The variation of stress with t in an Al/SiC FGM under free/free boundary conditions at $x = l/50$ (Figures 1(a), 18(b), $l = 5$ mm, $t_o = 0{\cdot}2$ μs).

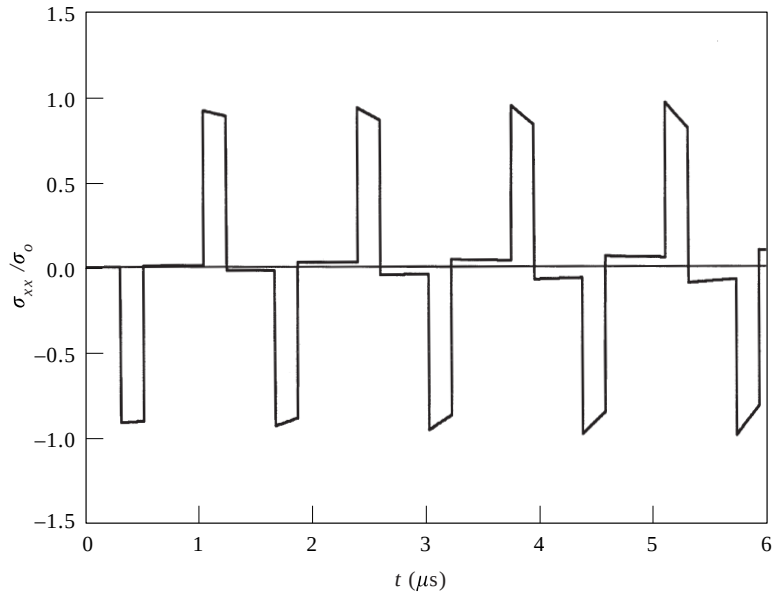

Figure 27. The variation of σ_{xx}/σ_o with t in an Al/SiC FGM under free/free boundary conditions at $x = l/2$ (Figures 1(a), 18(b), $l = 5$ mm, $t_o = 0{\cdot}2$ μs).

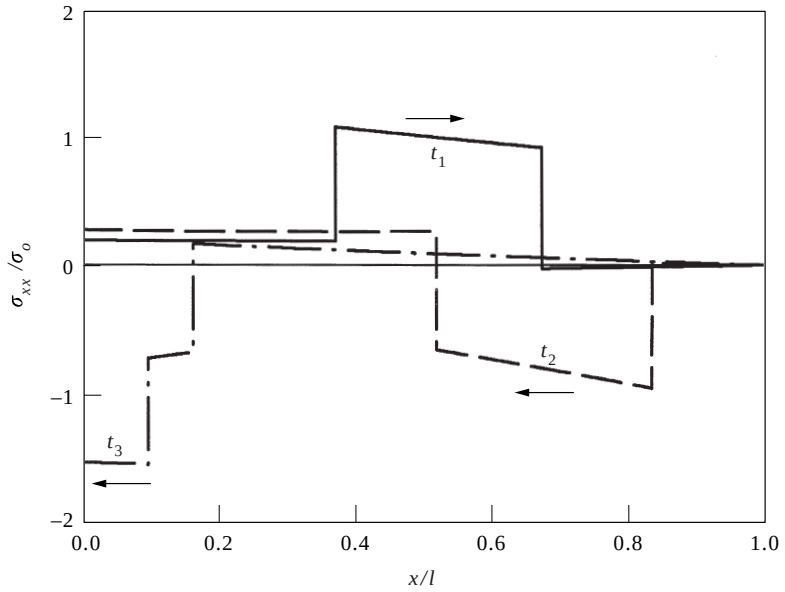

Figure 28. The variation of σ_{xx}/σ_o with x in an Al/SiC FGM under fixed/free boundary conditions at $t_1 = 2{\cdot}5$ μs, $t_2 = 3$ μs, and $t_3 = 3{\cdot}5$ μs; the arrows indicate the direction of pulse propagation (Figures 1(b), 18(b), $l = 5$ mm, $t_o = 0{\cdot}2$ μs).

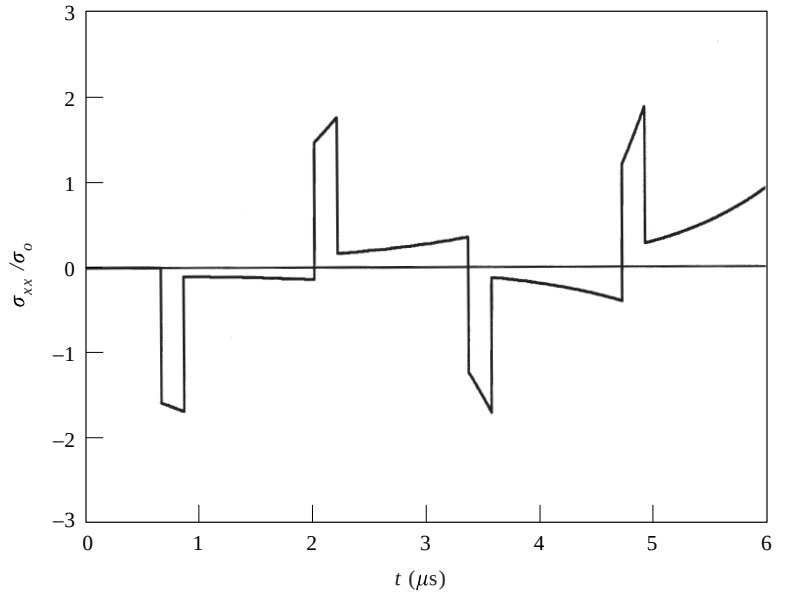

Figure 29. The variation of σ_{xx}/σ_o with t in an Al/SiC FGM under fixed/free boundary conditions at $x = 0$ (Figures 1(b), 18(b), $l = 5$ mm, $t_o = 0{\cdot}2$ μs).

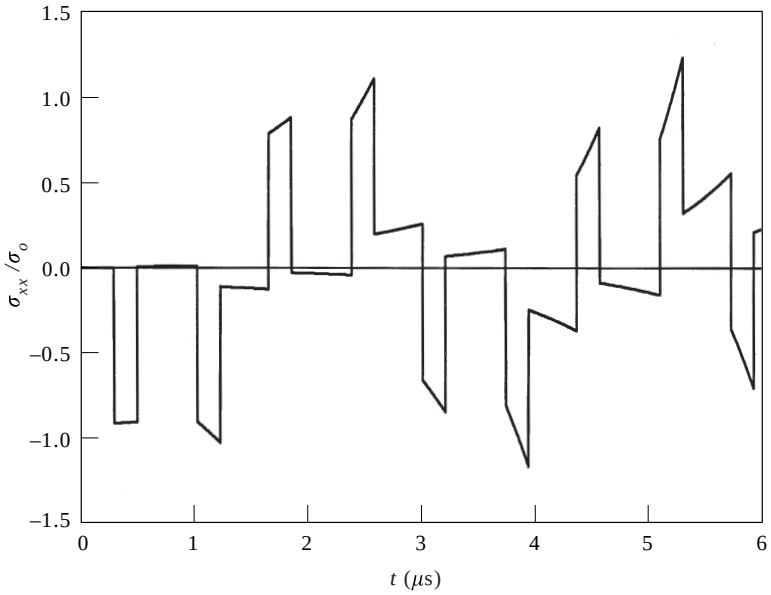

Figure 30. The variation of σ_{xx}/σ_o with t in an Al/SiC FGM under fixed/free boundary conditions at $x = l/2$ (Figures 1(b), 18(b), $l = 5$ mm, $t_o = 0{\cdot}2$ μs).

18(a) and (b), the normalized stress σ_{xx}/σ_o is given by Figures 19–24 and 25–30, respectively. The results of the two examples considered and the general expression given by equation (42) show that if the pulse is applied on the stiffer side of the graded medium, the amplitude ratio $\Delta\sigma/\sigma_o$ decreases in the thickness direction. Since in FGM coatings the surface subjected to the impact loading is usually stiffer, this general result indicates one of the advantages of graded coatings.

In the absence of an exact solution, as in, for example, problems with fixed/free boundaries, one may use the energy balance to examine the accuracy of the asymptotic solutions. Initially the medium is stress-free and is at rest, meaning that for $t \leqslant 0$ the elastic energy U_V and the kinetic energy U_T are zero. For $t > 0$, since the medium is non-dissipative, the energy balance principle requires that the sum of elastic and kinetic energies be equal to the work W of external loads, that is

$$W(t) = U_V(t) + U_T(t), \qquad t > 0. \tag{48}$$

In the FGM plate shown in Figure 1, for a unit surface area the external work is

$$W(t) = \int_0^t \sigma_{xx}(l, s)\, \mathrm{d}u(l, s), \tag{49}$$

where $\sigma_{xx}(l, t)$ is given by equation (40) and the transform of u is given by equation (11), which, for example, in a slab with fixed/free boundaries and for $m = n + 2$ may be expressed as

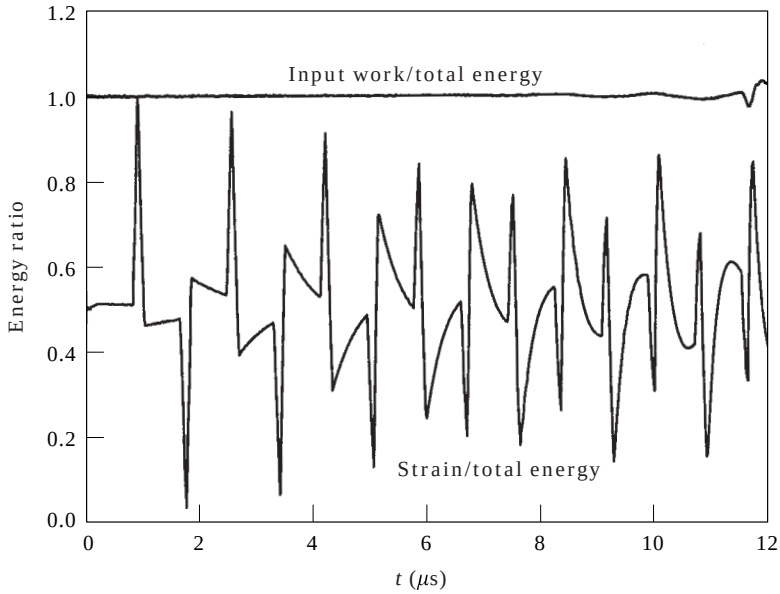

Figure 31. The energy balance in a Ni/ZrO_2 FGM slab under fixed/free boundary conditions subjected to the pulse $\sigma_{xx}(l, t) = -\sigma_o[H(t) - H(t - t_o)]$ (Figures 1(b), 2(a), $l = 5$ mm, $t_o = 0{\cdot}2$ μs).

$$\hat{U}(X,p) = \frac{\sigma_o \hat{f}(p)}{E_0'(a+1)^{n+2}a}\left[\frac{(aX+1)^{s_3} - (aX+1)^{s_4}}{s_3(a+1)^{s_3-1} - s_4(a+1)^{s_4-1}}\right]. \tag{50}$$

By inverting equation (50) for $X = 1$ (or $x = l$) and using equation (40), from equation (49) one obtains

$$\begin{aligned} W(t) &= -\sigma_o u(l,t), \qquad 0 < t \leqslant t_o, \\ &= -\sigma_o u(l,t_o), \qquad t > t_o. \end{aligned} \tag{51}$$

At time t the total strain energy in the medium (per unit surface area) may be obtained from

$$U_V(t) = \int_0^l \frac{\sigma_{xx}^2(x,t)}{2E'(x)}\,\mathrm{d}x, \tag{52}$$

where E' is given by equation (2) and σ_{xx} may be obtained by inverting equation (34) in wave summation form. Similarly, the total kinetic energy per unit surface area may be written as

$$U_T(t) = \int_0^l \frac{\rho(x)}{2}\left[\frac{\partial}{\partial t}u(x,t)\right]^2 \mathrm{d}x, \tag{53}$$

where ρ is given by equation (1) and the particle velocity $\partial u/\partial t$ is obtained from equation (50) by inverting $p\hat{U}(x/l, p)$, again in wave summation form.

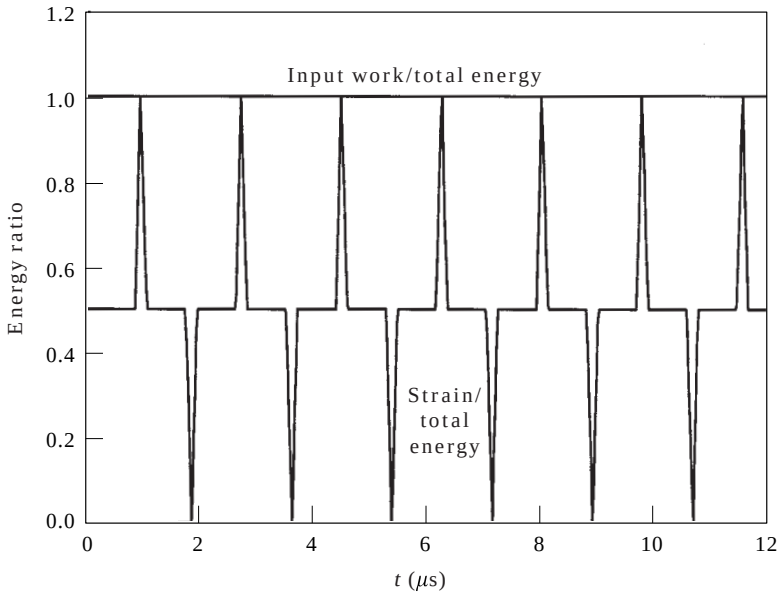

Figure 32. The energy balance in a homogeneous nickel slab under fixed/free boundary conditions subjected to the pulse $\sigma_{xx}(l, t) = -\sigma_o[H(t) - H(t - t_o)]$ (Figures 1(b), $l = 5$ mm, $t_o = 0{\cdot}2$ μs).

For the FGM plate considered in section 4.1 with fixed/free boundary conditions (Figure 1(b)) and the composition as shown in Figure 2(a), the energy balance is shown in Figure 31. Here the terminology "total energy" is used for $U_V(t) + U_T(t)$ calculated from equations (52) and (53). The "input work" $W(t)$ is calculated from equation (51). The figure shows $U_V/(U_V + U_T)$ and $W_V/(U_V + U_T)$. Theoretically one should have $W(t)/[U_V(t) + U_T(t)] = 1$. For reference, the energy balance in a pure Ni plate having the same dimension and under the same boundary conditions and external load as the FGM plate is shown in Figure 32. The similarity between the two results seems to disappear after the first few wave reflections. Despite this, Figure 31 shows that the agreement between theoretical and calculated total energies is nearly perfect up to 11 μs. For $t > 11$ μs there are signs of greater discrepancy between the two results, indicating that for longer values of time one needs to retain more than six terms in the asymptotic series giving the stress and the displacement.

Based on the results obtained in this study one may conclude that: (1) in an inhomogeneous plate under one-dimensional wave propagation the initial pulse shape may undergo considerable distortion which depends heavily on the boundary conditions and material composition; (2) the pulse duration remains unchanged; (3) the jump discontinuity in stress $\Delta\sigma$ is a function of location but not of time; (4) depending on the material property grading, $\Delta\sigma$ may be greater or less than σ_o, the amplitude of the input pulse; (5) as the pulse goes through there is an "overshoot" in stress which must be added to $\Delta\sigma$ in order to calculate the peak stress; (6) $\Delta\sigma/\sigma_o$ can be expressed in closed form as a simple function of

location; and (7) in the absence of an exact solution the energy balance principle may be used as a convergence criterion.

ACKNOWLEDGMENTS

This study was supported by AFOSR under the grant F49620-98-1-0028 and by ARO under the grant DAAHO4-95-1-0232.

REFERENCES

1. M. YAMANOUCHI, M. KOIZUMI, T. HIRAI and I. SHIOTA (editors) 1990 FGM '90, *Proceedings of the* lst *International Symposium on Functionally Gradient Materials*, Tokyo, Japan: FGM Forum.
2. J. B. HOLT, M. KOIZUMI, T. HIRAI and Z. A. MUNIR (editors) 1993 *Ceramic Transactions—Functionally Gradient Materials* **34** Westerville, Ohio: American Ceramic Society.
3. B. ILSCHNER and N. CHERRADI (editors) 1994 FGM 94, *Proceedings of the* 3*rd International Symposium on Structural and Functional Gradient Materials*. Lausaune, Switzerland: Presses Polytechniques et Universitaires Romandes.
4. I. SHIOTA and Y. MIYAMOTO (editors) 1997 FGM 96, *Functionally Graded Materials*. Amsterdam: Elsevier.
5. F. G. FRIEDLANDER 1946 *Proceedings of the Cambridge Philosophical Society, Mathematical and Physical Sciences* **43**, 360–373. Simple progressive solutions of the wave equations.
6. F. C. KARAL and J. B. KELLER 1959 *The Journal of the Acoustical Society of America* **31**, 694–705. Elastic wave propagation in homogeneous and inhomogeneous media.
7. C. L. PEKERIS 1946 *The Journal of the Acoustic Society of America* **18**, 295–315. Theory of propagation of sound in a half-space of variable sound velocity under conditions of formulation of a shadow zone.
8. J. G. J. SCHOLTE 1961 *Geophysical Prospecting* **9**, 86–115. Propagation of wave in inhomogeneous media.
9. R. N. GUPTA 1965 *Geophysics* **30**, 122–132. Reflection of plane waves from a linear transition layer in liquid media.
10. U. S. LINDHOLM and K. D. DOSHI 1965 *Journal of Applied Mechanics* **32**, 135–142. Wave propagation in an elastic nonhomogeneous bar of finite length.
11. E. L. REISS 1969 *Journal of Applied Mechanics* **36**, 803–808. One-dimensional impact waves in inhomogeneous elastic media.
12. E. L. REISS 1969 *SIAM Journal on Applied Mathematics* **17**, 526–542. The impact problem for the Klein–Gordan equation.
13. J. S. WHITTIER 1965 *Journal of Applied Mechanics* **32**, 947–949. A note on wave propagation in a nonhomogeneous bar.
14. R. G. PAYTON 1966 *The Quarterly Journal of Mechanics and Applied Mathematics* **19**, 83–91. Elastic wave propagation in a non-homogeneous rod.
15. C. R. STEELE 1969 *AIAA Journal* **7**, 896–902. Asymptotic analysis of stress waves in inhomogeneous elastic solids.
16. M. J. YEDLIN, B. R. SEYMOUR and B. C. ZELT 1987 *Geophysics* **52**, 755–764. Truncated asymptotic representation of waves in a one-dimensional elastic medium.
17. A. KARLSSON, H. OTTERHEIM and R. STEWART 1993 *Journal of the Optical Society of America A, Optics and Image Science* **10**, 886–895. Transient wave propagation in composite media: Green's function approach.
18. C. T. SUN, J. D. ACHENBACH and G. HERRMANN 1968 *Journal of Applied Mechanics* **35**, 467–473. Continuum theory for a laminated medium.

19. G. A. HEGEMIER and A. H. NAYFEH 1973 *Journal of Applied Mechanics* **40**, 503–510. A continuum theory for wave propagation in laminated composites. Case I: propagation normal to the laminates.
20. Z. P. DUAN, J. W. EISCHEN and G. HERRMANN 1986 *Journal of Applied Mechanics* **53**, 108–115. Harmonic wave propagation in nonhomogeneous layered composites.
21. D. M. PAI 1985 *Geophysics* **50**, 1541–1547. A new solution method for the wave equation in inhomogeneous media.
22. A. H. HARKER and J. A. OGILVY 1991 *Ultrasonics* **29**, 235–244. Coherent wave propagation in inhomogeneous materials: a comparison of theoretical models.
23. G. E. ROBERTS and H. KAUFMAN 1966 *Table of Laplace Transforms* Philadelphia: W. B. Saunders Company. See p. 251.
24. G. N. WATSON 1966 *A Treatise on the Theory of Bessel Functions*. New York: Cambridge University Press; 2nd edition. See pp. 202–203.

A: EXPRESSIONS OF THE FIRST SEVEN TERMS ($j=1, \ldots, 7$) OF α_{ikj} THAT APPEAR IN EQUATION (21), ($i=1, 2$; $k=0, 1, 2, \ldots$)

$$\alpha_{ik1} = -\frac{1}{8}(n+1)^2 a^2 b_{ik},$$

$$\alpha_{ik2} = \frac{1}{128}(n+1)^4 a^4 b_{ik}^2,$$

$$\alpha_{ik3} = \frac{1}{128}(n+1)^4 a^4 b_{ik} - \frac{1}{3072}(n+1)^6 a^6 b_{ik}^3,$$

$$\alpha_{ik4} = -\frac{1}{1024}(n+1)^6 a^6 b_{ik}^2 + \frac{1}{98\,304}(n+1)^8 a^8 b_{ik}^4,$$

$$\alpha_{ik5} = -\frac{1}{1024}(n+1)^6 a^6 b_{ik} + \frac{1}{16\,384}(n+1)^8 a^8 b_{ik}^3 - \frac{1}{3\,932\,160}(n+1)^{10} a^{10} b_{ik}^5,$$

$$\alpha_{ik6} = \frac{5}{32\,768}(n+1)^8 a^8 b_{ik}^2 - \frac{1}{393\,216}(n+1)^{10} a^{10} b_{ik}^4 + \frac{1}{188\,743\,680}(n+1)^{12} a^{12} b_{ik}^6,$$

$$\alpha_{ik7} = \frac{5}{32\,768}(n+1)^8 a^8 b_{ik} - \frac{3}{262\,144}(n+1)^{10} a^{10} b_{ik}^3 + \frac{1}{12\,582\,912}(n+1)^{12} a^{12} b_{ik}^5 - \frac{1}{10\,569\,646\,080}(n+1)^{14} a^{14} b_{ik}^7.$$

B: EXPRESSIONS OF THE FUNCTIONS W_{ix} AND W_{il}, $i = 1, \ldots, 4$

$$
\begin{aligned}
W_{1x} = {} & \left[\frac{\sqrt{2\pi z_o}}{e^{z_o}} I_{\nu-1}(z_o) + \frac{\sqrt{2\pi z_o}}{e^{z_o}} I_{\nu+1}(z_o)\right]\left[\sqrt{\frac{2z_x}{\pi}}\, e^{z_x} K_{\nu-1}(z_x) + \sqrt{\frac{2z_x}{\pi}}\, e^{z_x} K_{\nu+1}(z_x)\right] \\
& + \frac{2}{z_o}\left(\frac{m-1}{n-m+2}\right)\left(\frac{\sqrt{2\pi z_o}}{e^{z_o}} I_{\nu-1}(z_o)\right) \\
& \times \left[\sqrt{\frac{2z_x}{\pi}}\, e^{z_x} K_{\nu-1}(z_x) + \sqrt{\frac{2z_x}{\pi}}\, e^{z_x} K_{\nu+1}(z_x)\right] \\
& - \frac{2}{z_o}\left(\frac{m-1}{n-m+2}\right)(aX+1)^{\frac{m-n-2}{2}} \\
& \times e^{z_x} K_{\nu}(z_x))\left[\frac{\sqrt{2\pi z_o}}{e^{z_o}} I_{\nu-1}(z_o) + \frac{\sqrt{2\pi z_o}}{e^{z_o}} I_{\nu+1}(z_o)\right] \\
& - \frac{4}{z_o^2}\left(\frac{m-1}{n-m+2}\right)^2 (aX+1)^{\frac{m-n-2}{2}}\left(\frac{\sqrt{2\pi z_o}}{e^{z_o}} I_{\nu}(z_o)\right)\left(\sqrt{\frac{2z_x}{\pi}}\, e^{z_x} K_{\nu}(z_x)\right),
\end{aligned}
$$

$$
\begin{aligned}
W_{2x} = {} & \left[\frac{\sqrt{2\pi z_x}}{e^{z_x}} I_{\nu-1}(z_x) + \frac{\sqrt{2\pi z_x}}{e^{z_x}} I_{\nu+1}(z_x)\right] \\
& \times \left[\sqrt{\frac{2z_o}{\pi}}\, e^{z_o} K_{\nu-1}(z_o) \quad + \sqrt{\frac{2z_o}{\pi}}\, e^{z_o} K_{\nu+1}(z_o)\right] \\
& + \frac{2}{z_o}\left(\frac{m-1}{n-m+2}\right)\left(\frac{\sqrt{2\pi z_x}}{e^{z_x}} I_{\nu-1}(z_x)\right) \\
& \times \left[\sqrt{\frac{2z_o}{\pi}}\, e^{z_o} K_{\nu-1}(z_o) + \sqrt{\frac{2z_o}{\pi}}\, e^{z_o} K_{\nu+1}(z_o)\right] \\
& - \frac{2}{z_o}\left(\frac{m-1}{n-m+2}\right)(aX+1)^{\frac{m-n-2}{2}} \\
& \times \left(\sqrt{\frac{2z_o}{\pi}}\, e^{z_o} K_{\nu}(z_o)\right)\left[\frac{\sqrt{2\pi z_x}}{e^{z_x}} I_{\nu-1}(z_x) + \frac{\sqrt{2\pi z_x}}{e^{z_x}} I_{\nu+1}(z_x)\right] \\
& - \frac{4}{z_o^2}\left(\frac{m-1}{n-m+2}\right)^2 (aX+1)^{\frac{m-n-2}{2}}\left(\frac{\sqrt{2\pi z_x}}{e^{z_x}} I_{\nu}(z_x)\right)\left(\sqrt{\frac{2z_o}{\pi}}\, e^{z_o} K_{\nu}(z_o)\right),
\end{aligned}
$$

$$
\begin{aligned}
W_{3x} = {} & \left(\frac{\sqrt{2\pi z_o}}{e^{z_o}} I_{\nu}(z_o)\right)\left[\sqrt{\frac{2z_x}{\pi}}\, e^{z_x} K_{\nu-1}(z_x) + \sqrt{\frac{2z_x}{\pi}}\, e^{z_x} K_{\nu+1}(z_x)\right] \\
& - \frac{2}{z_o}\left(\frac{m-1}{n-m+2}\right)(aX+1)^{\frac{m-n-2}{2}}\left(\frac{\sqrt{2\pi z_o}}{e^{z_o}} I_{\nu}(z_o)\right)\left(\sqrt{\frac{2z_x}{\pi}}\, e^{z_x} K_{\nu}(z_x)\right),
\end{aligned}
$$

$$W_{4x} = \left(\sqrt{\frac{2z_o}{\pi}}\,\mathrm{e}^{z_o}\mathrm{K}_\nu(z_o)\right)\left[\frac{\sqrt{2z_x}}{\mathrm{e}^{z_x}}\mathrm{I}_{\nu-1}(z_x) + \frac{\sqrt{2\pi z_x}}{\mathrm{e}^{z_x}}\mathrm{I}_{\nu+1}(z_x)\right]$$
$$-\frac{2}{z_o}\left(\frac{m-1}{n-m+2}\right)(aX+1)^{\frac{m-n-2}{2}}\left(\frac{\sqrt{2\pi z_x}}{\mathrm{e}^{z_x}}\mathrm{I}_\nu(z_o)\right)\left(\sqrt{\frac{2z_o}{\pi}}\,\mathrm{e}^{z_o}\mathrm{K}_\nu(z_o)\right),$$

$$W_{1l} = \left[\frac{\sqrt{2\pi z_o}}{\mathrm{e}^{z_o}}\mathrm{I}_{\nu-1}(z_o) + \frac{\sqrt{2\pi z_o}}{\mathrm{e}^{z_o}}\mathrm{I}_{\nu+1}(z_o)\right]\left[\sqrt{\frac{2z_l}{\pi}}\,\mathrm{e}^{z_l}\mathrm{K}_{\nu-1}(z_l) + \sqrt{\frac{2z_l}{\pi}}\,\mathrm{e}^{z_l}\mathrm{K}_{\nu+1}(z_l)\right]$$
$$+\frac{2}{z_o}\left(\frac{m-1}{n-m+2}\right)\left(\frac{\sqrt{2\pi z_o}}{\mathrm{e}^{z_o}}\mathrm{I}_{\nu-1}(z_o)\right)\left[\sqrt{\frac{2z_l}{\pi}}\,\mathrm{e}^{z_l}\mathrm{K}_{\nu-1}(z_l) + \sqrt{\frac{2z_l}{\pi}}\,\mathrm{e}^{z_l}\mathrm{K}_{\nu+1}(z_l)\right]$$
$$-\frac{2}{z_o}\left(\frac{m-1}{n-m+2}\right)(a+1)^{\frac{m-n-2}{2}}\left(\sqrt{\frac{2z_l}{\pi}}\,\mathrm{e}^{z_l}\mathrm{K}_\nu(z_l)\right)$$
$$\times\left[\frac{\sqrt{2\pi z_o}}{\mathrm{e}^{z_o}}\mathrm{I}_{\nu-1}(z_o) + \frac{\sqrt{2\pi z_o}}{\mathrm{e}^{z_o}}\mathrm{I}_{\nu+1}(z_o)\right]$$
$$-\frac{4}{z_o^2}\left(\frac{m-1}{n-m+2}\right)^2(a+1)^{\frac{m-n-2}{2}}\left(\frac{\sqrt{2\pi z_o}}{\mathrm{e}^{z_o}}\,\mathrm{I}_\nu(z_o)\right)\left(\sqrt{\frac{2z_l}{\pi}}\,\mathrm{e}^{z_l}\mathrm{K}_\nu(z_l)\right),$$

$$W_{2l} = \left[\frac{\sqrt{2\pi z_l}}{\mathrm{e}^{z_l}}\mathrm{I}_{\nu-1}(z_l) + \frac{\sqrt{2\pi z_l}}{\mathrm{e}^{z_l}}\mathrm{I}_{\nu+1}(z_l)\right]\left[\sqrt{\frac{2z_o}{\pi}}\,\mathrm{e}^{z_o}\mathrm{K}_{\nu-1}(z_o) + \sqrt{\frac{2z_o}{\pi}}\,\mathrm{e}^{z_o}\mathrm{K}_{\nu+1}(z_o)\right]$$
$$+\frac{2}{z_o}\left(\frac{m-1}{n-m+2}\right)\left(\frac{\sqrt{2\pi z_l}}{\mathrm{e}^{z_l}}\mathrm{I}_{\nu-1}(z_l)\right)\left[\sqrt{\frac{2z_o}{\pi}}\,\mathrm{e}^{z_o}\mathrm{K}_{\nu-1}(z_o) + \sqrt{\frac{2z_o}{\pi}}\,\mathrm{e}^{z_o}\mathrm{K}_{\nu+1}(z_o)\right]$$
$$-\frac{2}{z_o}\left(\frac{m-1}{n-m+2}\right)(a+1)^{\frac{m-n-2}{2}}\left(\sqrt{\frac{2z_o}{\pi}}\,\mathrm{e}^{z_o}\mathrm{K}_\nu(z_o)\right)$$
$$\times\left[\frac{\sqrt{2\pi z_l}}{\mathrm{e}^{z_l}}\mathrm{I}_{\nu-1}(z_l) + \frac{\sqrt{2\pi z_l}}{\mathrm{e}^{z_l}}\mathrm{I}_{\nu+1}(z_l)\right]$$
$$-\frac{4}{z_o^2}\left(\frac{m-1}{n-m+2}\right)^2(a+1)^{\frac{m-n-2}{2}}\left(\frac{\sqrt{2\pi z_l}}{\mathrm{e}^{z_l}}\,\mathrm{I}_\nu(z_l)\right)\left(\sqrt{\frac{2z_o}{\pi}}\,\mathrm{e}^{z_o}\mathrm{K}_\nu(z_o)\right),$$

$$W_{3l} = \left(\frac{\sqrt{2\pi z_o}}{\mathrm{e}^{z_o}}\mathrm{I}_\nu(z_o)\right)\left[\sqrt{\frac{2z_l}{\pi}}\,\mathrm{e}^{z_l}\mathrm{K}_{\nu-1}(z_l) + \sqrt{\frac{2z_l}{\pi}}\,\mathrm{e}^{z_l}\mathrm{K}_{\nu+1}(z_l)\right]$$
$$-\frac{2}{z_o}\left(\frac{m-1}{n-m+2}\right)(a+1)^{\frac{m-n-2}{2}}\left(\frac{\sqrt{2\pi z_o}}{\mathrm{e}^{z_o}}\mathrm{I}_\nu(z_o)\right)\left(\sqrt{\frac{2z_l}{\pi}}\,\mathrm{e}^{z_l}\mathrm{K}_\nu(z_l)\right),$$

$$W_{4l} = \left(\sqrt{\frac{2z_o}{\pi}}\,\mathrm{e}^{z_0}\mathrm{K}_\nu(z_o)\right)\left[\frac{\sqrt{2\pi z_l}}{\mathrm{e}^{z_l}}\mathrm{I}_{\nu-1}(z_l) + \frac{\sqrt{2\pi z_l}}{\mathrm{e}^{z_l}}\mathrm{I}_{\nu+1}(z_l)\right]$$
$$-\frac{2}{z_o}\left(\frac{m-1}{n-m+2}\right)(a+1)^{\frac{m-n-2}{2}}\left(\frac{\sqrt{2\pi z_l}}{\mathrm{e}^{z_l}}\mathrm{I}_\nu(z_l)\right)\left(\sqrt{\frac{2z_o}{\pi}}\,\mathrm{e}^{z_o}\mathrm{K}_\nu(z_o)\right),$$

where $\nu = |(1-m)/(n-m+2)|$ and z_o, z_l, and z_x are given by equation (27).

C: WAVE PROPAGATION IN AN INHOMOGENEOUS MEDIUM WITH A CONSTANT SPEED OF SOUND

If the speed of sound in an inhomogeneous slab is constant, approximating the material parameters by

$$E'(x) = E'_o\mathrm{e}^{\alpha x}, \qquad \rho(x) = \rho_o\mathrm{e}^{\alpha x}, \qquad c = \sqrt{E'_o/\rho_o}, \tag{C1}$$

for free/free boundary conditions the solution may be obtained as

$$\hat{u}(x,p) = \frac{\sigma_o\hat{f}(p)}{E'_o\mathrm{e}^{\alpha l}}\left[\frac{s_2\mathrm{e}^{s_1 x} - s_1\mathrm{e}^{s_2 x}}{s_1 s_2(\mathrm{e}^{s_1 l} - \mathrm{e}^{s_2 l})}\right], \tag{C2}$$

$$s_1, s_2 = -\frac{\alpha}{2} \pm \sqrt{\left(\frac{\alpha}{2}\right)^2 + \left(\frac{p}{c}\right)^2}. \tag{C3}$$

The exact and the first term asymptotic solutions for the stress may then be expressed as

$$\frac{\sigma_{xx}(x,t)}{\sigma_o} = \mathrm{e}^{-\frac{\alpha}{2}(l-x)} *$$
$$\times \sum_{k=0}^{\infty}\left\{\left[f(t-\theta_{1k}) - \frac{\alpha c\theta_{1k}}{2}\int_0^{\sqrt{t^2-\theta_{1k}^2}} f(t-\sqrt{\tau^2+\theta_{1k}^2})\frac{\mathrm{J}_1\left(\frac{\alpha c}{2}\tau\right)}{\sqrt{\tau^2+\theta_{1k}^2}}\,\mathrm{d}\tau\right]\right.$$
$$\times \mathrm{H}(t-\theta_{1k}) - \left[f(t-\theta_{2k}) - \frac{\alpha c\theta_{2k}}{2}\int_0^{\sqrt{t^2-\theta_{2k}^2}} f(t-\sqrt{\tau^2+\theta_{2k}^2})\right.$$
$$\left.\left.\times \frac{\mathrm{J}_1\left(\frac{\alpha c}{2}\tau\right)}{\sqrt{\tau^2+\theta_{2k}^2}}\,\mathrm{d}\tau\right]\mathrm{H}(t-\theta_{2k})\right\},$$
$$\theta_{1k} = [(2k+1)l - x]/c, \qquad \theta_{2k} = [(2k+1)l + x]/c, \tag{C4}$$

and

$$\frac{\sigma_{xx}(x,t)}{\sigma_o} \cong \mathrm{e}^{-\frac{\alpha}{2}(l-x)}\sum_{k=0}^{\infty}[f(t-\theta_{1k})\mathrm{H}(t-\theta_{1k}) - f(t-\theta_{2k})\mathrm{H}(t-\theta_{2k})]. \tag{C5}$$